arXiv:0711.4234v1 [cond-mat.dis-nn] 27 Nov 2007

Magnetotransport of electrons in quantum Hall systems

I.A. Dmitriev[1,*], **F. Evers**[1], **I.V. Gornyi**[1,*], **A.D. Mirlin**[1,2,†], **D.G. Polyakov**[1], and **P. Wölfle**[2,1]

[1] Institut für Nanotechnologie, Forschungszentrum Karlsruhe, 76021 Karlsruhe, Germany
[2] Institut für Theorie der Kondensierten Materie, Universität Karlsruhe, 76128 Karlsruhe, Germany

Key words Quantum Hall systems, magnetotransport, Landau quantization, magneto-oscillations, disorder, magnetoresistance, memory effects, electron-electron interaction, Coulomb drag, photoconductivity
PACS 73.21.-b, 73.43.-f, 73.43.Qt, 73.50.Jt, 73.63.-b, 73.50.Pz

Recent theoretical results on magnetotransport of electrons in a 2D system in the range of moderately strong transverse magnetic fields are reviewed. The phenomena discussed include: quasiclassical memory effects in systems with various types of disorder, transport in lateral superlattices, interaction-induced quantum magnetoresistance, quantum magnetooscillations in *dc* and *ac* transport, and oscillatory microwave photoconductivity.

Copyright line will be provided by the publisher

1 Introduction

Electronic transport in semiconductor nanostructures is one of the central issues of research in modern condensed matter physics, see, *e.g.*, [1, 2] for reviews. In this article, we review recent results on transport of two-dimensional electron gases (2DEG) in moderately strong transverse magnetic fields B. Specifically, we concentrate on a range of B which are classically strong (i.e., $\omega_c\tau_{\rm tr} \gg 1$, where ω_c is the cyclotron frequency and $\tau_{\rm tr}$ the transport relaxation time), but where quantum localization effects (and, correspondingly, quantum Hall physics) are not developed yet. There exists a broad class of phenomena that lead to strong magnetoresistivity $\rho_{xx}(B)$ in this range of fields, in view of the developed cyclotron motion. These phenomena are discussed in the present review.

2 Quasiclassical memory effects in magnetoresistance

The recent interest in *quasiclassical* transport properties of a 2DEG has been largely motivated by the experimental and practical importance of high-mobility heterostructures, in which charged impurities are separated from the 2DEG by a wide spacer. The correlation radius of disorder produced by the impurities is usually much larger than the Fermi wave length of electrons and transport in the 2DEG retains signatures of the underlying quasiclassical dynamics of the particles. On the theoretical side, much of the interest has been inspired by a variety of anomalous transport phenomena which, while being essentially classical, cannot be described by Boltzmann-Drude kinetic theory. The quasiclassical "non-Boltzmann" phenomena in disordered electron systems are due to correlations of scattering acts at the points where quasiclassical paths self-intersect, which gives rise to *memory effects*, neglected in the conventional Boltzmann equation. In particular, the non-Markovian kinetics yields a strong magnetoresistance (MR) and anomalies in the ac response. The strength of the quasiclassical anomalies depends on the ratio d/l, where d is the correlation radius of disorder, l the mean free path, and grows with increasing d as a power of this parameter. Since quantum corrections (weak localization, Altshuler-Aronov corrections, etc.) are governed by a different small parameter $1/k_F l \ll 1$, where k_F is the Fermi wave vector, it is the long-range correlations of disorder

---

[*] Also at A.F. Ioffe Physico-Technical Institute, 194021 St. Petersburg, Russia
[†] Also at St.Petersburg Nuclear Physics Institute, 188300 St.Petersburg, Russia.

with $k_F d \gg 1$ that reveal the quasiclassical anomalies. In this section, we focus on the quasiclassical memory effects in magnetotransport.

2.1 Magnetoresistance of a 2DEG subject to smooth disorder

We begin by considering the MR of a 2DEG in the presence of Gaussian disorder which is smooth on the scale of k_F^{-1}. First of all, we recall that there exists a finite MR [3, 4] even within the collision-integral approximation, the source of which is the bending of quasiclassical trajectories by magnetic field B on the scale of the correlation radius d. This leads to a small negative MR, $\Delta\rho_{xx}/\rho_0 \sim -(d/R_c)^2$, where ρ_0 is the Drude resistivity and R_c is the cyclotron radius. Remarkably, the non-Markovian kinetics gives rise to a much stronger positive MR [5], which may even be much larger than unity.

To systematically treat the quasiclassical memory effects, the starting point is the disorder-averaged expression for the conductivity tensor σ in terms of the exact Liouville operator L:

$$\sigma = e^2\nu v_F^2 \int \frac{d\phi}{2\pi} \left\langle \begin{pmatrix} \cos\phi \\ \sin\phi \end{pmatrix} L^{-1} \begin{pmatrix} \cos\phi \\ \sin\phi \end{pmatrix}^T \right\rangle . \tag{1}$$

Here ν is the density of states, v_F the Fermi velocity, ϕ the velocity angle on the Fermi surface. The operator $L = L_0 + \delta L$ is given by the sum of the free part $L_0 = -i\omega + v_F \mathbf{n}\nabla + \omega_c\partial_\phi$, where ω_c is the cyclotron frequency, $\mathbf{n} = (\cos\phi, \sin\phi)$, and the part induced by a random scalar potential $V(\mathbf{r})$,

$$\delta L = \delta v(\mathbf{r})\mathbf{n}\nabla + [\nabla\delta v(\mathbf{r})](\hat{\mathbf{z}} \times \mathbf{n})\partial_\phi \ , \tag{2}$$

where $\delta v(\mathbf{r}) = v(\mathbf{r}) - v_F$ denotes a fluctuation of the local Fermi velocity $v(\mathbf{r}) = [v_F^2 - 2V(\mathbf{r})/m)]^{1/2}$ and $\hat{\mathbf{z}}$ is a unit vector in z direction. Expanding Eq. (1) in δL, averaging over the disorder and resumming the series, the diagonal resistivity $\rho_{xx} = 2(-i\omega + M_{xx})/e^2\nu v_F^2$ is represented in terms of the disorder-induced self-energy ("memory function") M_{xx}.

The Drude result $M_{xx}^{(0)} = \tau_{\text{tr}}^{-1}$, where τ_{tr} is the momentum relaxation time, follows as the first term in a perturbative expansion of the self-energy in the strength of disorder, $M_{xx}^{(0)} = -\langle \delta L\ L_0^{-1}\ \delta L\rangle$. Substituting the propagator L_{D}^{-1} renormalized by impurity scattering for L_0^{-1} in the latter expression yields the main contribution to the MR associated with the quasiclassical memory effects. When calculating L_{D}^{-1} in the case of long-range disorder, the stochastic motion of particles can be approximated by a Fokker-Planck equation corresponding to the diffusion in momentum space, so that L_{D} is written as

$$L_{\text{D}} = -i\omega + v_F\mathbf{n}\nabla + \omega_c\partial_\phi - \tau_{\text{tr}}^{-1}\partial_\phi^2 \ . \tag{3}$$

The leading correction to M_{xx} due to the self-intersection of quasiclassical paths then reads:

$$\Delta M_{xx} = (4\pi^3 m^2 v_F^2)^{-1} \int d^2q\, d\phi\, \sin\phi\, \sin(\phi - \phi_q) q^2 W(q)\, g_{\text{D}}(\omega, \mathbf{q}, \phi) \ , \tag{4}$$

where $g_{\text{D}}(\omega, \mathbf{q}, \phi)$ is the Fourier-transformed real-space solution of the equation $L_{\text{D}} g_{\text{D}} = \sin\phi \sin(\phi - \phi_q)\delta(\mathbf{r})$, ϕ_q is the angle of $\mathbf{q}$, and $W(q)$ is the Fourier transform of the correlator $\langle V(0)V(\mathbf{r})\rangle$. For the case of impurities separated from the 2DEG by a spacer of width d, Eq. (4) gives [5]

$$\Delta\rho_{xx}/\rho_0 = \Delta M_{xx}/M_{xx}^{(0)} = 2\pi^{-1}\zeta(3/2)\,(d/l)^3\,(\omega_c\tau_{\text{tr}})^{9/2} \ . \tag{5}$$

One sees that the MR due to the memory effects is much larger than that related to the effect of magnetic field on the collision integral for $\omega_c\tau_{\text{tr}} \gg (l/d)^{2/5}$. The MR (5) becomes of order unity when the mean-square shift of the guiding center of a cyclotron orbit after one revolution,

$$\delta = 2\pi^{1/2} v_F\tau_{\text{tr}}/(\omega_c\tau_{\text{tr}})^{3/2}, \tag{6}$$

becomes of order d, which happens at $\omega_c\tau_{\text{tr}} \sim (l/d)^{2/3}$. At higher fields, the strong positive MR is followed by a sharp (exponential) falloff of ρ_{xx} with growing B [6]:

$$\ln(\rho_{xx}/\rho_0) \sim -(d/\delta)^{2/3} , \tag{7}$$

which is due to the increasing adiabaticity of the electron dynamics and the related quasiclassical localization. The self-intersection induced MR, given by Eq. (5), may be considered as a precursor of the adiabatic localization.

In the limit of weak inhomogeneities, the return-induced MR depends in an essential way on the behavior of the disorder under time reversal [5]; in particular, it is strongly enhanced in a random magnetic field (RMF). The case of a smoothly varying RMF is of particular interest in view of the composite-fermion description of the transport properties of a half-filled Landau level [7]. Also, a long-range RMF has been realized in semiconductor heterostructures by attaching superconducting or ferromagnetic overlayers or by “prepatterning” the sample (randomly curving the 2DEG layer). Following the same route as for the case of a random scalar potential, the MR due to the quasiclassical memory effects is obtained as [5]

$$\rho_{xx}/\rho_0 = 1/2 + [1/4 + (B/B_0)^2]^{1/2} , \tag{8}$$

where B_0 is the characteristic amplitude of fluctuations of the RMF. For the composite-fermion model at half-filling, $(B/B_0)^2$ is represented as $2(d/l)(\omega_c\tau_{\text{tr}})^2$. The adiabatic localization in the RMF begins at $B \sim B_0(l/d)^{1/6}$ [8], so that there is a wide range of B in which the positive MR (8) is strong.

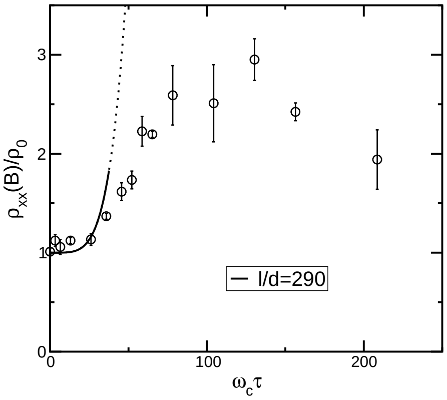

Fig. 1 Magnetoresistivity in a random potential from numerical simulations in comparison with Eq. (5) for $l/d = 290$.

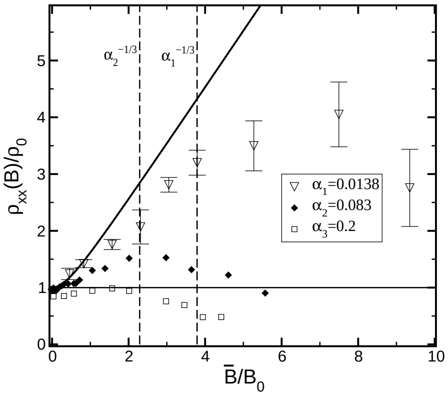

Fig. 2 Magnetoresistivity in a random magnetic field from numerical simulations for three different strengths of the disorder $\alpha = (eB_0/mc)(d/v_F)$; the full line corresponds to Eq. (8).

The numerically calculated MR [5] for both types of disorder shown in Figs. 1 and 2 confirm the theoretically predicted positive MR. Note that the MR in the RMF at moderately small d/l still exists, but becomes weak; this is the region of d/l relevant to the composite-fermion model. The numerical data for $d/l \sim 0.1 - 0.2$ agree well [8] with the experimental results [9] for the MR around half-filling. Recent unpublished numerical simulations [10] also confirm the $\omega_c^{9/2}$ positive MR in a smooth potential; however, the numerical coefficient is found [10] to be smaller by a factor ~ 2 as compared to Eq. (5).

2.2 Magnetoresistance of a 2DEG subject to two-component disorder

We now turn to a 2DEG moving in a non-Gaussian random potential represented by rare strong short-range scatterers and subject additionally to a smooth random potential discussed in Sec. 2.1. One of the most relevant experimental realizations of the model of “two-component disorder” is random antidot (AD) arrays, where the potential barriers around the ADs can be modeled as hard disks reflecting electrons specularly (for experimental work on the dc MR in random AD arrays see, e.g., Refs. [11, 12, 13, 14, 15, 16]). The model is also applicable to the description of the MR in an unstructured ultra-high mobility 2DEG with a wide spacer, where large-angle scattering on residual interface impurities and interface roughness becomes important [17, 18, 19], limiting the mobility with further increasing width of the spacer. From the theoretical point of view, the interplay of the two types of inhomogeneities is quite remarkable in that it yields nontrivial physics which is absent in the limiting cases, when only one type is present. In particular, although in the extreme of strong $B \to \infty$ the resistivity ρ_{xx} tends to zero in either of the limiting cases, it diverges in the presence of both types of disorder [20]. Also, in the experimentally relevant situation when the mean free path at zero B is determined by scattering on ADs, the presence of weak long-range disorder will nonetheless become of crucial importance with increasing B [21, 20]. The magnetotransport in the Lorentz-gas model describing an AD array without smooth disorder has been studied, in particular, in Refs. [22, 23, 24, 25, 26]. A strong negative MR followed by a metal-insulator phase transition in a strong magnetic field was found in [22, 23, 25]; the low-field anomalous MR due to the "corridor effect" was investigated in [26]. Smooth disorder, however, changes the MR qualitatively, as discussed below.

Generalizing the formalism described in Sec. 2.1 to the case of two-scale disorder, we represent the Liouville operator as $L = L_{\rm D} + \delta L$, where $L_{\rm D}$ is given by Eq. (3) and includes interaction with the smooth disorder ($\tau_{\rm sm}$ is the corresponding transport scattering time), whereas $\delta L = -\sum_i I_{\mathbf{R}_i}$ describes collisions with ADs whose random positions are $\mathbf{R}_i$. The Fourier transform $\tilde{I}_q$ of the collision operator $I_{\mathbf{R}_i}$ yields the transport time τ_S for the scattering by the AD array of density n_S through $\tilde{I}_0\mathbf{n} = -\mathbf{n}/n_S\tau_S$. We assume that $\omega_c^{-1} \ll \tau_S \ll \tau_{\rm sm}$, so that the total transport rate is determined by ADs, $\tau_{\rm tr}^{-1} = \tau_S^{-1} + \tau_{\rm sm}^{-1} \simeq \tau_S^{-1}$. The leading contribution to ΔM_{xx} reads

$$\Delta M_{xx} = -n_S \textstyle\int (d\phi/\pi) \cos\phi \, I_{\mathbf{R}} D I_{\mathbf{R}} \, \cos\phi \ , \tag{9}$$

where the propagator D includes the first-order self-energy: $D = (L_{\rm D} - n_S\tilde{I}_0)^{-1}$. As compared to the Lorentz model [27] in which only hard-disk scatterers are present, new physics emerges in the limit $\delta \gg a$, where a is the radius of the ADs and δ is the shift of the cyclotron orbit after one revolution due to scattering on smooth disorder (cf. Sec. 2.1). In particular, Eq. (9) yields [21]

$$\Delta\rho_{xx}/\rho_0 = -(\omega_c/\omega_0)^2 \ , \quad \omega_0 = (2\pi n_S)^{1/2} v_F (3\tau_S/2\tau_{\rm sm})^{1/4} \ , \tag{10}$$

for $\omega_c \ll \omega_0$. The mechanism of the negative MR (10) can be understood as follows. If one associates with a particle trajectory a strip of width $2a$, the ratio $(\omega_c/\omega_0)^2$ gives the fraction of the area "explored" twice, which implies an effective reduction of the exploration rate and thus a longer time between collisions with *different* ADs. The negative MR (10) should be contrasted with the positive MR (5) for one-scale smooth disorder, where the passages through the same area lead to an enhanced scattering rate.

For $\omega_c \gg \omega_0$, the renormalized scattering time $\tau'_S \gg \tau_S$ should be found self-consistently from the condition $n_S \xi R_c \sim 1$, where $\xi \sim \delta(v_F\tau'_S/R_c)^{1/2}$ is a characteristic end-to-end size of the diffusive guiding-center trajectory in time τ'_S, which gives the B^{-4} falloff [21] with increasing B:

$$\rho_{xx}/\rho_0 \sim \tau_S/\tau'_S \sim (\tau_S/\tau_{\rm sm})(n_S R_c^2)^2 \ . \tag{11}$$

Equation (11) is valid as long as $\tau'_S \ll \tau_{\rm sm}$, which is rewritten as $n_S R_c^2 \gg 1$. In the opposite limit (but still for $\delta \ll d$), the scattering on ADs stops playing any role and ρ_{xx} has a plateau with

$$\rho_{xx}/\rho_0 = \tau_S/\tau_{\rm sm} \ . \tag{12}$$

Let us now briefly outline what happens at larger B, namely for $\delta/d \ll 1$ [20]. In dilute AD arrays for intermediate B, the exponential slowdown of the electron dynamics induced by adiabatic localization transforms into $\rho_{xx}/\rho_0 \sim n_S R_c d \ln(1/n_S R_c d) \propto B^{-1}\ln B$ due to rare collisions with ADs which mix otherwise closed drift trajectories in phase space. Most interesting, however, is the behavior of ρ_{xx} in the limit of large B, where ρ_{xx} starts to grow as a power law with increasing B. This behavior can be most clearly seen in a "hydrodynamic model" of the chaotic AD array ($n_S \to \infty$, $\tau_S = \mathrm{const}$), where the problem can be mapped onto that of advection-diffusion transport [28]. In the limit $B \to \infty$ the hydrodynamic model predicts $\rho_{xx}/\rho_0 \sim (\tau_S^2 v_F d/\tau_{\text{sm}} R_c^2)^{5/13} \propto B^{10/13}$. The physics of the positive MR is a percolation of drifting cyclotron orbits limited by scattering on ADs. The growth is checked on the side of large B by quantum effects (Shubnikov-de Haas oscillations). The different types of the MR in the two-component model [20] are illustrated in Fig. 3 for various concentrations of short-range scatterers (ADs): (i) the MR is positive owing to the "diffusion-controlled percolation"; (ii) due to the adiabatic localization, the concentration of conducting electrons decreases as $B^{-1} \ln B$ before the percolation becomes effective, which yields a negative MR $\rho_{xx}(B) \propto B^{-1} \ln B$ for intermediate B; (iii) an exponentially sharp falloff of $\rho_{xx}(B)$ at $B \sim B_{ad}$ (shown as a vertical jump) separates the diffusive and drift regimes; (iv) because of the memory effects, the collision time for scattering by ADs is increased as compared to the Drude value already in the diffusive regime ($B \ll B_{ad}$), which leads to the negative MR $\rho_{xx}(B) \propto B^{-4}$ for small B; (v) for intermediate B, the scattering on ADs stops playing any role and $\rho_{xx}(B)$ is saturated at a value determined by the long-range disorder only, whereas at larger fields the diffusion-controlled percolation gives rise to a positive MR.

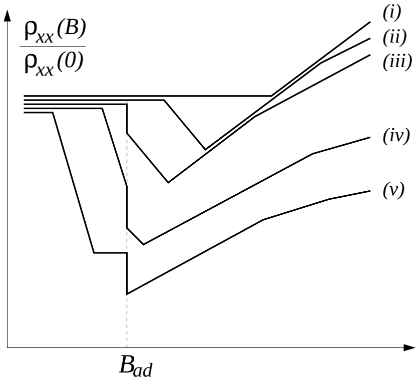

Fig. 3 Schematic behavior of the magnetoresistivity $\rho_{xx}(B)$ on a log-log scale in the two-component disorder model for different values of the concentration of antidots n: $n^{(i)} > n^{(ii)} > \ldots > n^{(v)}$, keeping all other parameters ($\tau_S, \tau_{\text{sm}}, d$) fixed. Only one characteristic field B_{ad} is shown, at which the crossover between diffusive dynamics and adiabatic drift in the long-range potential takes place.

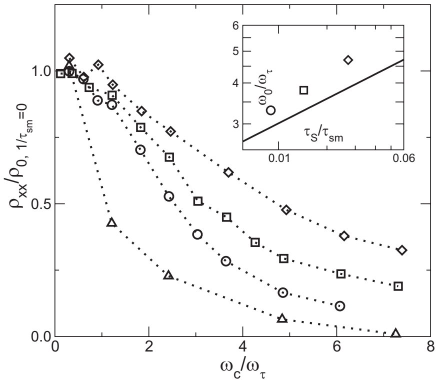

Fig. 4 Magnetoresistivity in a two-component-disorder model at fixed τ_S and different τ_{sm} from numerical simulations; $\tau_{\text{sm}}/\tau_S = \infty$ (Lorentz gas, △), 111 (◯), 70 (□), 37 (◇). Inset: ω_0 determined from the fit to the quadratic behavior given by Eq. (10); the full line corresponds to the analytical result for ω_0 from Eq. (10).

The MR obtained numerically [21] for the model of two-scale disorder in the regime of Eqs. (10)-(12), Fig. 4, shows good agreement with the above analytical results. As far as the experimental data are concerned, for typical parameters [13] of AD arrays, $n_S = (0.6\,\mu\mathrm{m})^{-2}$, $v_F \tau_S = 1.3\,\mu\mathrm{m}$, $v_F \tau_{\text{sm}} = 16\,\mu\mathrm{m}$, and the electron density $5 \times 10^{11}\,\mathrm{cm}^{-2}$, the field B_0 corresponding to the frequency ω_0 given by Eq. (10) is $\simeq 0.3\,T$, in agreement with the experimental findings [13]. A similar negative MR was reported in Refs. [11, 12, 14]. For ultra-high mobility samples [electron density $2 \times 10^{11}\,\mathrm{cm}^{-2}$, $v_F \tau_S \simeq 80\,\mu\mathrm{m}$, $\tau_{\text{sm}}/\tau_S \sim 10$, $a \sim 10\,\mathrm{nm}$, $n_S \sim (2\,\mu\mathrm{m})^{-2}$ [18]], one gets $B_0 \sim 60\,\mathrm{mT}$. A strong negative MR has indeed been observed [19, 29] in the very-high-mobility heterostructures, in qualitative agreement with the above theory.

2.3 Quasiclassical memory effects in ac magnetotransport

In addition to the strong MR, the non-Markovian quasiclassical kinetics in the presence of long-range disorder gives rise to an anomalous ac response. In particular, the return-induced correction to the ac conductivity $\mathrm{Re}\,\sigma(\omega)$ exhibits a kink [30] $\propto |\omega|$ at $\omega \to 0$. The quasiclassical zero-frequency anomaly is not sensitive to inelastic scattering (in contrast to the weak-localization quantum correction) but manifests itself only [31] in the presence of an external metallic gate that screens the long-range Coulomb interaction. As outlined below, in a strong B, the diagonal ac conductivity $\mathrm{Re}\,\sigma_{xx}(\omega)$ shows pronounced resonant features [32, 33] on top of the cyclotron resonance (CR), which are induced by the memory effects.

In the Lorentz model (hard disks with no smooth disorder), which is intended to mimic a random AD array in heterostructures in the limit of a large spacer, the shape of the CR is very different from the Lorentzian and not characterized by the Drude scattering rate [24, 32]. Altogether, the behavior of $\mathrm{Re}\,\sigma_{xx}(\omega)$ associated with quasiclassical cyclotron orbits skipping around the ADs turns out to be remarkably rich [32]. The skipping-orbit contribution is broadened on a scale of ω_c and vanishes at ω_c in a nonanalytical way as $|\omega - \omega_c|$. Apart from these two features, $\mathrm{Re}\,\sigma_{xx}(\omega)$ for moderately strong B with $R_c \gg a$ oscillates with a period ω_c up to $\omega = \omega_c R_c/a$ and shows a series of square-root spikes for larger ω. The modulation yields exact zeros of the ac response at the harmonics of the CR.

Adding a smooth random potential, present in typical heterostructures, changes the above picture in an essential way. Following the formalism of Sec. 2.2, the classical return-induced contribution to the real part of the oscillatory ac conductivity $\sigma_\omega^{(c)}$ is represented for $\tau_S \ll \tau_{\rm sm}$ and $\delta \gg d$ as [33]

$$\sigma_\omega^{(c)}/\sigma_\omega^{\rm D} = -\mathrm{Re}\,P_\omega/n_S\tau_S\ , \qquad P_\omega = \sum\nolimits_{n=1}^{\infty}\int dt\, e^{-i\omega t - t/\tau_S}\, p_n[\,0, v_F(t-2\pi n/\omega_c)\,]\ , \tag{13}$$

where $\sigma_\omega^{\rm D}$ is the real part of the dynamic Drude conductivity, Eq. (30). In Eq. (13), the function $p_n(x_\perp, x_\parallel) = (3^{1/2}\pi n^2\delta^2)^{-1}\exp\left[-(3x_\perp^2 + x_\parallel^2)/3n\delta^2\right]$ describes the electron distribution in time $t = 2\pi n/\omega_c$ after n cyclotron revolutions along $(x_\parallel)$ and across $(x_\perp)$ the cyclotron orbit. In the case of a weak damping of the quasiclassical magnetooscillations, $\sigma_\omega^{(c)}$ is represented as a series of sharp dips at $\omega = N\omega_c$, whose amplitude and width are of order $\sigma^{\rm D}(a/N\delta)(\omega_c\tau)^{1/2}$ and $\tau_S^{-1} + N^2\tau_{\rm sm}^{-1}$, respectively. In the regime of harmonic oscillations (exponential damping), $\sigma_\omega^{(c)}$ is written as [33]

$$\sigma_\omega^{(c)}/\sigma_\omega^{\rm D} = 1 - (a/\pi^{1/2}\delta)\,\cos(2\pi\omega/\omega_c)\,\exp\left[-(\omega/\omega_c)^2(3\pi/\omega_c\tau_{\rm sm})\right]\ . \tag{14}$$

It is worth stressing that these oscillations are of essentially classical origin and have nothing to do with the Landau quantization. The behavior of $\sigma_\omega^{(c)}$ is illustrated in Fig. 5, where also the quantum oscillations $\propto \exp(-2\pi/\omega_c\tau_q)$, with τ_q being the single-particle (quantum) relaxation time, are shown. One sees that the classical oscillations may be stronger than the quantum ones since in high-mobility structures $\tau_q \ll \tau_{\rm sm}$ and the quantum oscillations are damped much more strongly.

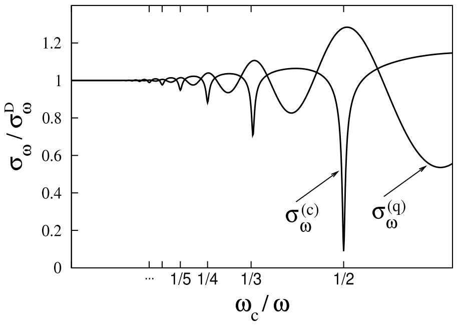

Fig. 5 Quasiclassical [$\sigma_\omega^{(c)}$, Eq. (14)] and quantum [$\sigma_\omega^{(q)}$] oscillatory ac conductivity (normalized to the Drude conductivity $\sigma_\omega^{\rm D}$) vs ω_c/ω for $\omega/2\pi = 100$ GHz, $\tau_{\rm sm} = 0.6$ ns, $\tau_{\rm sm}/\tau_{\rm q} = 50$, $\tau_S/\tau_{\rm sm} = 0.1$, $a/\delta = 0.25$ at $\omega_c/\omega = 1/2$.

3 Magnetotransport in modulated systems (lateral superlattices)

3.1 Weiss oscillations in one-dimensional superlattices

Transport properties of a two-dimensional electron gas (2DEG) subject to a periodic potential (lateral superlattice) with a period much shorter than the electron transport mean free path (but much larger than the Fermi wave length) have been intensively studied during the last decade. In a pioneering experiment [34] Weiss *et al.* discovered that a weak one-dimensional (1D) modulation with wave vector $\mathbf{q} \parallel \mathbf{e}_x$ induces strong commensurability oscillations of the magnetoresistivity $\rho_{xx}(B)$ (while showing almost no effect on $\rho_{yy}(B)$ and $\rho_{xy}(B)$), with the minima satisfying the condition $2R_c/a = n - 1/4$, $n = 1, 2, \ldots$, where R_c is the cyclotron radius and $a = 2\pi/q$ the modulation wave length. The quasiclassical nature of these commensurability oscillations was demonstrated by Beenakker [35], who showed that the interplay of the cyclotron motion and the superlattice potential induces a drift of the guiding center along y axis, with an amplitude squared oscillating as $\cos^2(qR_c - \pi/4)$ (this is also reproduced by a quantum-mechanical calculation, see [36]). While describing nicely the period and the phase of the experimentally observed oscillations, the result of [35], however, failed to explain the observed rapid decay of the oscillation amplitude with decreasing magnetic field. The cause for this discrepancy was in the treatment of disorder: while Ref. [35] assumed isotropic impurity scattering, in experimentally relevant high-mobility semiconductor heterostructures the random potential is very smooth and induces predominantly small-angle scattering, with the total relaxation rate $\tau_{\rm q}^{-1}$ much exceeding the momentum relaxation rate $\tau_{\rm tr}^{-1}$. The theory of commensurability oscillations in one-dimensional modulation, $V(x) = \eta E_F \cos qx$ with $\eta \ll 1$, in the situation of smooth disorder was worked out in [37].

The starting point is the Boltzmann equation for the distribution function $F(x, \mathbf{n})$ of electrons,

$$\mathcal{L}F(x,\mathbf{n}) = -ev(x)\mathbf{E}\mathbf{n}\ ; \qquad \mathcal{L} = v(x)\mathbf{n}\partial_{\mathbf{r}} + \omega_c\partial_\phi - \sin\phi\, v'(x)\partial_\phi - C\ , \tag{15}$$

where $\mathbf{n} = (\cos\phi, \sin\phi)$ is the direction and $v(x) = [2m(E_F + eU(x))]^{1/2}$ the magnitude of the Fermi velocity, and C is the collision integral. The resulting modulation-induced contribution to resistivity reads [37]

$$\frac{\Delta\rho_{xx}}{\rho_0} = \frac{\eta^2 ql}{4} Q \frac{\pi}{\sinh\pi\mu} J_{i\mu}(Q) J_{-i\mu}(Q)\ ; \qquad \mu = \frac{Q}{qv_F\tau_{\rm q}}\left[1 - \left(1 + \frac{\tau_{\rm q}}{\tau_{\rm tr}}Q^2\right)^{-1/2}\right]\ , \tag{16}$$

where we introduced the dimensionless parameter $Q = qR_c$ convenient to characterize the strength of the magnetic field. At low magnetic fields, $Q \gg Q_{\rm dis}$, with $Q_{\rm dis} = (2ql/\pi)^{1/3}$, the oscillations are exponentially damped by disorder, and the magnetoresistivity saturates at the value $\Delta\rho_{xx}/\rho_0 = \eta^2 ql/4$. (At still lower magnetic fields, $Q > Q_{\rm ch}$, with $Q_{\rm ch} = 2/\eta$, and for a sufficiently strong modulation, $\eta^{3/2}ql \gg 1$, an additional strong magnetoresistivity occurs, dominated by the channeled orbits, see Sec. 3.3.) In strong fields, $Q \ll Q_{\rm dis}$, the amplitude of oscillations increases as B^3,

$$\Delta\rho_{xx}/\rho_0 = [(\eta ql)^2/\pi Q^3]\cos^2(Q - \pi/4)\ . \tag{17}$$

In Fig. 6 the theoretical results are compared with experimental data of Weiss *et al* [34]. The sample parameters are [34] $q = 2\pi/382\text{nm}$, $n_e = 3.16 \times 10^{11}\text{cm}^{-2}$, $\tau_{\rm tr} = 52\text{ps}$, the total relaxation rate is taken to be $\tau_{\rm q}^{-1} = (3\text{ps})^{-1}$. As is seen from the figure, with the modulation strength $\eta = 0.065$ a very good description of the experimentally observed magnetoresistivity is obtained. (At lowest B, the experimental data show positive magnetoresistance discussed in Sec. 3.3.) The difference between the long-range potential scattering and the isotropic scattering is illustrated in the right panel, where the results for the modulation-induced $\Delta\rho_{xx}$ are plotted for both models of disorder at the same value of $\tau_{\rm tr}$. As was shown in [38], modulation-induced commensurability oscillations can be also observed in attenuation and velocity change of a surface acoustic wave propagating near a 2DEG.

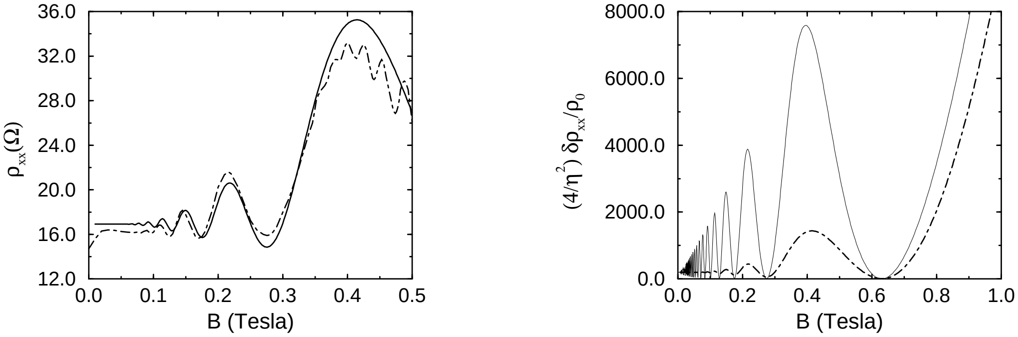

Fig. 6 Weiss oscillations in a 1D superlattice. *Left panel:* Experimental data of Ref.[34] (dash-dotted line) compared with the theoretical results for the long-range potential scattering (full line). Parameters are: $q = 2\pi/382$nm, $n_e = 3.16 \times 10^{11}\mathrm{cm}^{-2}$, $\tau = 52$ps, $\tau_s = 3$ps, $\eta = 0.065$. *Right panel:* Grating-induced correction to the 2DEG reistivity, $\Delta\rho_{xx}/\rho_0$, in units of $\eta^2/4$ for the isotropic potential scattering ($\tau_{\mathrm{tr}} = 52$ps, full line) and the long-range random potential scattering ($\tau_{\mathrm{tr}} = 52$ps, $\tau_{\mathrm{q}} = 3$ps, dash-dotted line). The sample parameters ($q = 2\pi/382$nm, $n_e = 3.16 \times 10^{11}\mathrm{cm}^{-2}$) are the same as in Ref.[34].

In [39] Weiss oscillations were studied for the vicintiy of the $\nu = 1/2$ filling of the lowest Landau level; see also related works [40, 41]. Within the composite fermion theory, the problem is described in terms of fermions subject to a spatially modulated magnetic field and scattered by a random magnetic field. The magnetic character of modulation shifts the phase of Weiss oscillations, while the random magnetic fields considerably enhances their damping. The obtained results are in agreement with experimental studies [42, 43], which confirms the validity of the composite-fermion description of the $\nu = 1/2$ state.

3.2 Two-dimensional superlattices

Magnetotransport in 2D superlattices with small-angle impurity scattering was studied in [44]. It was shown that the shape of the magnetoresistivity depends crucially on the parameter $\gamma = \eta^2 ql/4$.

For small γ (corresponding typically to a modulation strength not exceeding a few percent) the magnetoresistivity is given by the perturbative formulas (16) – (17) (the same as in 1D superlattices) up to the point $Q \sim Q_{\mathrm{P}} \equiv [0.13(\eta ql)^2]^{1/3}$, where the correction $\Delta\rho_{xx}$ becomes of the order of the Drude resistivity ρ_0. For higher magnetic fields the Péclet number $P \sim \eta ql/(qR_c)^{3/2}$ characterizing the advection-diffusion problem becomes large and the transport is determined by a narrow boundary layer around a square network of separatrices. As a result, the B^3-dependence of the oscillation amplitude characteristic for the perturbative ($Q > Q_{\mathrm{P}}$) regime crosses over to a much slower $B^{3/4}$-increase at $Q < Q_{\mathrm{P}}$,

$$\Delta\rho_{xx}/\rho_0 = (8\pi)^{1/4} C(\eta ql)^{1/2} Q^{-3/4} |\cos(Q - \pi/4)|^{1/2} \; . \tag{18}$$

For $\gamma \gg 1$ (which is typically valid for the modulation strength η larger than $10 \div 15\%$) the oscillations are damped at low magnetic fields not by disorder (as in the perturbative regime) but by the modulation-induced chaotic diffusion. The oscillations become observable at $Q \sim Q_{\mathrm{ad}} \equiv (4\pi/\eta^2)^{1/3}$ where the motion of electrons in the superlattice potential acquires the form of adiabatic drift. Since the violation of adiabaticity is exponentially small, the magnetoresistivity drops exponentially in a logarithmically narrow interval of magnetic fields, $Q'_{\mathrm{ad}} \equiv Q_{\mathrm{ad}}(\ln\gamma)^{-2/3} < Q < Q_{\mathrm{ad}}$,

$$\Delta\rho_{xx}/\rho_0 \propto \exp[-(\pi/2\sqrt{2}|\cos(Q - \pi/4)|)(Q_{\mathrm{ad}}/Q)^{3/2}] \; . \tag{19}$$

At higher magnetic fields the impurity scattering starts to dominate over the non-adiabatic processes and thus to determine the diffusion constant of the advection-diffusion problem, so that the commensurability oscillations take the same form (18) as in the large-P limit of the $\gamma \ll 1$ regime.

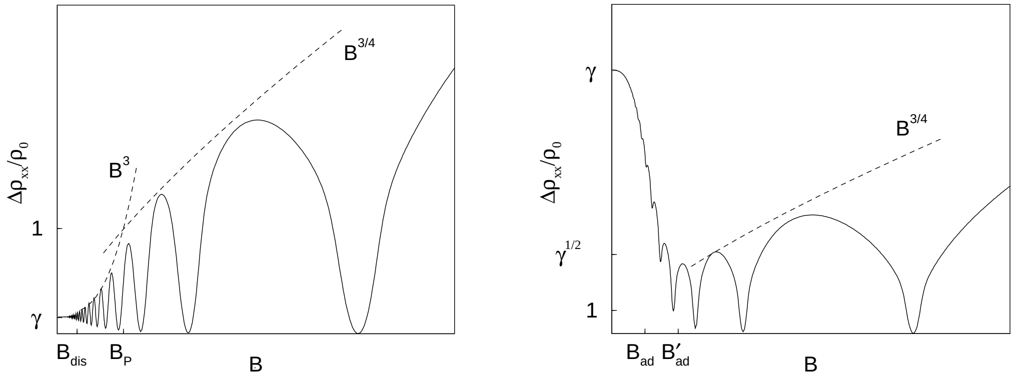

Fig. 7 *Left panel:* Schematic representation of the magnetoresistivity $\Delta\rho_{xx}(B)$ induced by a 2D modulation in the case $\gamma \ll 1$. Characteristic points $B_{\rm dis}$ and B_P on the magnetic field axis (corresponding to $Q = Q_{\rm dis}$ and $Q = Q_P$, see the text) are shown. Below $B_{\rm dis}$ the oscillations are exponentially damped and the magnetoresistivity saturates at $\Delta\rho_{xx} = \gamma$, while at $B = B_{\rm P}$ the B^3-behavior of $\Delta\rho_{xx}$ changes to a much slower, $B^{3/4}$-increase. *Right panel:* Schematic representation of $\Delta\rho_{xx}(B)$ in the case $\gamma \gg 1$. The magnetoresistivity starts to drop exponentially and the commensurability oscillation appear at the value $B_{\rm ad}$ of the magnetic field where the motion in the periodic potential takes the form of an adiabatic drift. At $B \sim B'_{\rm ad}$ the disorder starts to dominate over the non-adiabatic effects, leading to a $B^{3/4}$-increase of the oscillation amplitude.

3.3 Low-field magnetoresistance

A distinct low-field magnetoresistivity was observed, along with the commensurability oscillations, in the original experiment [34], as well as in numerous later experiments on the transport in a lateral superlattice. Specifically, in low magnetic fields B a positive magnetoresistivity was found, followed by a maximum in $\rho_{xx}(B)$. For not too strong modulation, the relevant magnetic fields are much weaker than those where the Weiss oscillations are observed, so that the two effects can be easily separated. Soon after the first experimental observation it was understood [47] (see also [46]) that the low-field magnetoresistivity is related to the existence of open (channeled) orbits in the magnetic fields $B < B_c = (\eta c/2e)qmv_F$. It is worth mentioning that this effect, which is not found within the η-expansion used in Refs. [35, 37], has its counterpart in the context of the sound absorption in metals in the presence of a magnetic field. There, the trapping of electrons in channeled orbits by a sound wave leads to non-linearity of the acoustic response of an electron gas, as was observed experimentally [48] and analyzed theoretically [49].

A quantitative analytical description of the problem in the presence of disorder was worked out in [45]. It was found that for a suffuciently strong modulation, $\eta^{3/2}ql \gg 1$, the contribution of channeled orbits to resistivity has the form

$$\Delta\rho_{xx}^{\rm ch}/\rho_0 = (\sqrt{2}/\pi^2)\eta^{7/2}(ql)^2 F_{\rm ch}(\beta) \;, \tag{20}$$

where $\beta = B/B_c$ and $F_{\rm ch}(\beta)$ is a parameterless function shown in the left panel of Fig. 8. This induces a low-field magnetoresistance that scales as $\eta^{7/2}$ with the modulation strength. It was further shown in [45] that the contribution of non-channeled orbits is also modified at $B \lesssim B_c$,

$$\Delta\rho_{xx}^{\rm nc}/\rho_0 = 2\pi\omega_c\tau\langle v_d^2\rangle/v_F^2 = (\eta^2/2\pi)qlF_{\rm nc}(B/B_c) \;, \tag{21}$$

where the dimensionless function $F_{\rm nc}(\beta)$ is shown in the middle panel of Fig. 8. In the right panel of Fig. 8 the theoretical results are compared with experimental data of Ref. [50].

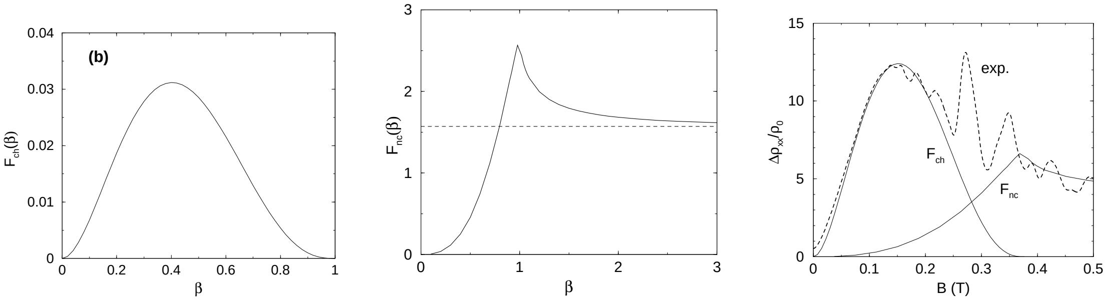

Fig. 8 *Left panel:* Function $F_{\rm ch}(\beta)$ describing magnetic field dependence of the contribution of channeled orbits to the resistivity. *Middle panel:* Function $F_{\rm nc}(\beta)$ characterizing the magnetic field dependence of the contribution of non-channeled orbits to resistivity. The dashed line indicates the asymptotic value $F_{\rm nc}(\beta \gg 1) = \pi/2$. *Right panel:* Experimental data for the low-field magnetoresistivity from Ref. [50] (dashed curve) compared to the theoretical results for the contributions of channeled [Eq.(21)] and non-channeled [Eq.(20)] orbits. The characteristic field B_c and the modulation amplitude found from the fit are $B_c \simeq 0.37$ T and $\eta \simeq 0.16$.

4 Interaction-induced magnetoresistance in non-quantizing fields

As discussed in Sec. 2, the longitudinal resistivity of an isotropic degenerate system is B–independent within the Drude-Boltzmann theory, $\rho_{xx}(B) = \rho_0 = (e^2\nu v_F^2\tau_{\rm tr})^{-1}$, where ν_0 is the density of states per spin. There are several distinct sources of a non-trivial MR, which reflect the rich physics of 2D systems. First, quasiclassical memory effects may lead to a MR(see Sec.2), which shows no T-dependence at low temperatures. Second, weak localization [51] induces a negative quantum MR restricted to the range of weak magnetic fields. Another quantum-mechanical source of the MR is electron–electron interaction. This type of the MR is the subject of the present Section.

It was discovered by Altshuler and Aronov [51] that the Coulomb interaction enhanced by the diffusive motion of electrons gives rise to a quantum correction to conductivity, which has in 2D the form $\delta\sigma_{xx} \simeq (e^2/2\pi^2)\ln T\tau_{\rm tr}$ (it is assumed here for simplicity that $\kappa \ll k_F$, where $\kappa = 4\pi e^2\nu_0$ is the inverse screening length; we also set $k_B = \hbar = 1$). The condition $T\tau_{\rm tr} \ll 1$ under which this result is derived [51] implies that electrons move diffusively on the time scale $1/T$ and is termed the "diffusive regime". Subsequent work [52] showed that in a strong magnetic field this correction (in combination with $\delta\sigma_{xy} = 0$) gives rise to a parabolic interaction–induced quantum MR,

$$\delta\rho_{xx}(B)/\rho_0 \simeq [(\omega_c\tau_{\rm tr})^2 - 1](\pi k_F l)^{-1}\ln T\tau_{\rm tr}, \qquad T\tau_{\rm tr} \ll 1, \tag{22}$$

where $\omega_c = eB/mc$ is the cyclotron frequency and $l = v_F\tau_{\rm tr}$ the transport mean free path.

The effect of interaction on the conductivity in the "ballistic regime" $T > 1/\tau_{\rm tr}$ has attracted a great deal of interest in a context of 2D systems showing a seemingly metallic behavior, $d\rho/dT > 0$ [53, 54]. Zala, Narozhny, and Aleiner [55] developed a systematic theory of the interaction corrections valid for arbitrary $T\tau_{\rm tr}$. In the ballistic range of temperatures, this theory predicts a linear-in-T correction to conductivity σ_{xx} and a $1/T$ correction to the Hall coefficient ρ_{xy}/B at $B \to 0$, and describes the MR in a *parallel* field. The consideration of [55] is restricted, however, to *classically weak* transverse fields, $\omega_c\tau_{\rm tr} \ll 1$, and to the *white-noise* disorder.

In this Section, we present a general theory of the interaction–induced corrections to the conductivity tensor of 2D electrons valid for arbitrary T, B and type of disorder [56]. A general expression for $\delta\sigma_{\alpha\beta}$ is derived in terms of the ballistic propagator $D(\omega, \mathbf{q}; \mathbf{n}, \mathbf{n}')$ describing the quasiclassical propagation of an electron in the phase space ($\mathbf{n}$ is the unit vector characterizing the direction of velocity on the Fermi surface). The result for the exchange contribution reads

$$\delta\sigma_{\alpha\beta} = -2e^2 v_{\rm F}^2\nu_0 \int_{-\infty}^{\infty}\frac{d\omega}{2\pi}\frac{\partial}{\partial\omega}\left\{\omega\coth\frac{\omega}{2T}\right\}\int\frac{d^2\mathbf{q}}{(2\pi)^2}\,{\rm Im}\left[\,U(\omega,\mathbf{q})\;B_{\alpha\beta}(\omega,\mathbf{q})\,\right], \tag{23}$$

where $U(\omega, \mathbf{q})$ is the interaction potential equal to a constant U_0 for point-like interaction and to $U(\omega, \mathbf{q}) = 2\pi e^2\{q + \kappa[1 + i\omega\langle D(\omega, q)\rangle]\}^{-1}$ for screened Coulomb interaction. The angular brackets $\langle \dots \rangle$ denote averaging over velocity directions $\mathbf{n}, \mathbf{n}'$. The tensor $B_{\alpha\beta}(\omega, \mathbf{q})$ is given by

$$\begin{aligned} B_{\alpha\beta}(\omega, \mathbf{q}) &= T_{\alpha\gamma}\pi\nu_0[\langle DS_{\gamma\delta}D\rangle - 2\langle Dn_\gamma Wn_\delta D\rangle]T_{\delta\beta} + T_{\alpha\gamma}\left(\delta_{\gamma\delta}\langle D\rangle/2 - \langle n_\gamma Dn_\delta\rangle\right)T_{\delta\beta} \\ &- 2T_{\alpha\gamma}\langle n_\gamma Dn_\beta D\rangle - \langle Dn_\alpha Dn_\beta D\rangle, \end{aligned} \tag{24}$$

where $T_{\alpha\beta} = 2\,\langle n_\alpha Dn_\beta\rangle|_{q=0,\omega\to 0} = \sigma_{\alpha\beta}/e^2v_F^2\nu_0$, $S_{xx} = S_{yy} = W(\mathbf{n}, \mathbf{n}')$, $S_{xy} = -S_{yx} = \omega_c/2\pi\nu_0$, and $W(\mathbf{n}, \mathbf{n}')$ is the impurity scattering cross-section. At $B \to 0$ one recovers the results for $\delta\sigma_{xx}$ and ρ_{xy} obtained in a different way in [55] for a white-noise disorder. Needless to say, in the diffusive limit, Eqs. (23), (24) reproduce (for arbitrary B and disorder range) the logarithmic correction (22).

The structure of Eqs. (23), (24) implies that the interaction correction is governed by returns of a particle to the original point in a time $t < T^{-1} \ll \tau_{\text{tr}}$. In a smooth random potential with a correlation length $d \gg k_F^{-1}$ the return probability is exponentially suppressed for $t \ll \tau_{\text{tr}}$. Therefore, the interaction correction in the ballistic regime is exponentially small at $B = 0$ for the case of smooth disorder. Moreover, the same argument applies to the case of a non-zero B, as long as $\omega_c \ll T$.

The situation changes qualitatively in a strong B, $\omega_c \gg T, \tau_{\text{tr}}^{-1}$: the particle experiences within the time $t \sim T^{-1}$ multiple cyclotron returns to the region close to the starting point. The MR is then determined by the correction to σ_{xx}. For the Coulomb interaction, the exchange contribution to the MR is given by

$$\delta\rho_{xx}/\rho_0 = -(\omega_c\tau_{\text{tr}})^2 G_F(T\tau_{\text{tr}})/\pi k_F l. \tag{25}$$

For the point-like interaction a similar result is obtained, with the replacement $G_F(T\tau_{\text{tr}}) \to \nu_0 U_0 G_0(T\tau_{\text{tr}})$. The functions $G_0(T\tau_{\text{tr}})$ and $G_F(T\tau_{\text{tr}})$, governing the T-dependence of the MR, are shown in Fig. 9. In the diffusive ($T\tau_{\text{tr}} \ll 1$) and ballistic ($T\tau_{\text{tr}} \gg 1$) limits they have the following asymptotics

$$G_0(x) \simeq \begin{cases} -\ln x + \text{const}, & x \ll 1, \\ c_0 x^{-1/2}, & x \gg 1, \end{cases} \qquad G_{\text{F}}(x) \simeq \begin{cases} -\ln x + \text{const}, & x \ll 1, \\ c_0 x^{-1/2}/2, & x \gg 1, \end{cases} \tag{26}$$

where $c_0 = 3\zeta(3/2)/16\sqrt{\pi} \simeq 0.276$

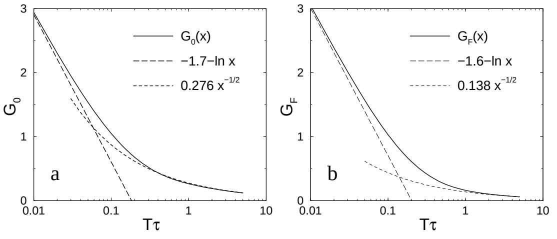

Fig. 9 Functions $G_0(T\tau_{\text{tr}})$ (a) and $G_{\text{F}}(T\tau_{\text{tr}})$ (b) determining the T-dependence of the exchange term for point-like and Coulomb interaction, respectively, Eq. (26).

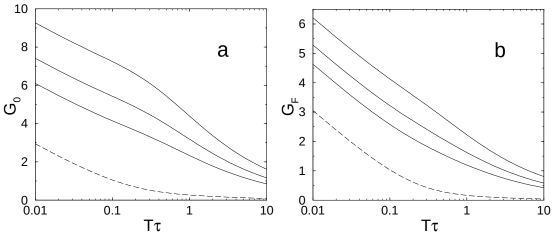

Fig. 10 Functions $G_0^{\text{mix}}(T\tau_{\text{tr}})$ (a) and $G_F^{\text{mix}}(T\tau_{\text{tr}})$ (b) describing the T dependence of the MR for point-like and Coulomb interaction, respectively, in the mixed-disorder model for different values of parameter $\gamma \equiv \tau_{\text{sm}}/\tau_{\text{tr}} = 20,\ 10,\ 5$ (from top to bottom). Dashed curves represent these functions for purely smooth disorder ($\gamma = 1$).

We turn now to the Hartree term, assuming $\kappa \ll k_F$. The expression for its triplet part is analogous to (23) with the replacement of $U(\omega, \mathbf{q})$ by $-\frac{3}{2}U(0, 2k_F\sin[(\phi - \phi')/2])$, where ϕ and ϕ' are the angles of the electron velocity. As to the singlet part, it is renormalized by mixing with the exchange term. The total

Hartree contribution (see Fig. 2) reads

$$\frac{\delta\rho_{xx}^{\mathrm{H}}(B)}{\rho_0} = frac(\omega_c\tau_{\mathrm{tr}})^2\pi^2 k_F l \begin{cases} y\ln y\left[\frac{3}{4}\ln(T\tau_{\mathrm{tr}}) + \ln y\right], & T\tau_{\mathrm{tr}} \ll 1, \\ y\ln^2[y(T\tau_{\mathrm{tr}})^{1/2}], & 1 \ll T\tau_{\mathrm{tr}} \ll (k_F/\kappa)^2, \\ \pi c_0(T\tau_{\mathrm{tr}})^{-1/2}, & T\tau_{\mathrm{tr}} \gg (k_F/\kappa)^2. \end{cases} \tag{27}$$

If κ/k_F is not small, the exchange contribution remains unchanged, while the Hartree term is subject to strong Fermi-liquid renormalization [51, 55] and is determined by angular harmonics $F_m^{\sigma,\rho}$ of the Fermi-liquid interaction $F^{\sigma,\rho}(\theta)$. The theoretically predicted $T^{-1/2}$ dependence of the interaction-induced MR has been observed in a high-mobility n-GaAs heterostructure with the smooth disorder [57].

Calculation of the correction $\delta\rho_{xy}$ to the Hall resistivity requires evaluation of both $\delta\sigma_{xx}$ and $\delta\sigma_{xy}$. The temperature dependence of $\delta\rho_{xy}$ in a strong B is governed by $\delta\sigma_{xx}$ in the diffusive limit and by $\delta\sigma_{xy}$ in the ballistic limit. For the point-like interaction, we find

$$\delta\rho_{xy}/\rho_{xy} = \nu_0 U_0 G_0^{\rho_{xy}}(T\tau_{\mathrm{tr}})/\pi k_F l, \qquad G_0^{\rho_{xy}}(x) = \begin{cases} -2\ln x + \mathrm{const}, & x \ll 1, \\ -11c_1 x^{1/2}, & x \gg 1, \end{cases} \tag{28}$$

with $c_1 = -\sqrt{\pi}\zeta(1/2)/4 \simeq 0.647$. An analogous consideration for the Coulomb interaction yields a similar result for the exchange correction (Fig. 11)

$$\delta\rho_{xy}^{\mathrm{F}}/\rho_{xy} = G_{\mathrm{F}}^{\rho_{xy}}(T\tau_{\mathrm{tr}})/\pi k_F l, \qquad G_{\mathrm{F}}^{\rho_{xy}}(x) = \begin{cases} -2\ln x + \mathrm{const}, & x \ll 1, \\ -(11/2)c_1 x^{1/2}, & x \gg 1. \end{cases} \tag{29}$$

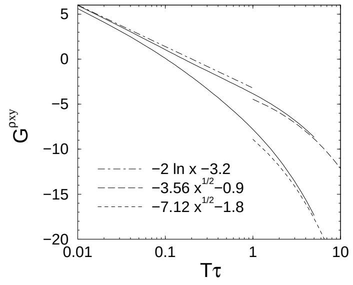

Fig. 11 Functions $G_0^{\rho_{xy}}(T\tau_{\mathrm{tr}})$ (lower curve)and $G_F^{\rho_{xy}}(T\tau_{\mathrm{tr}})$ (upper curve) describing the temperature dependence of the Hall resistivity for point-like and Coulomb interaction, respectively. Diffusive ($x \ll 1$) and ballistic ($x \gg 1$) asymptotics are also shown.

Above the interaction correction for a system with a small-angle scattering induced by smooth disorder with correlation length $d \gg k_F^{-1}$ has been studied. This is a typical situation for high-mobility GaAs structures with sufficiently large spacer d. It is known, however, that with further increasing width of the spacer the large-angle scattering on residual impurities and interface roughness becomes important and limits the mobility (see Sec. 2.2). Furthermore, in Si-based structures the transport relaxation rate is usually governed by scattering on short-range impurities. This suggests considering the two-component model of disorder: white-noise random potential with a mean free time τ_{wn} and a smooth random potential with a transport relaxation time τ_{sm}. It is assumed that while the transport relaxation rate $\tau_{\mathrm{tr}}^{-1} = \tau_{\mathrm{wn}}^{-1} + \tau_{\mathrm{sm}}^{-1}$ is governed by short-range disorder, $\tau_{\mathrm{wn}} \ll \tau_{\mathrm{sm}}$, the damping of SdHO is dominated by smooth random potential. This allows one to consider the range of classically strong magnetic fields, $\omega_c\tau_{\mathrm{wn}} \gg 1$, neglecting at the same time Landau quantization.

The presence of short-range scatterers enhances the MR as compared to the case of smooth disorder. For the point-like interaction the MR reads

$$\frac{\delta\rho_{xx}(B)}{\rho_0} = -\frac{(\omega_c\tau_{\mathrm{tr}})^2\nu_0 U_0}{\pi k_F l} G_0^{\mathrm{mix}}\left(T\tau_{\mathrm{tr}}, \frac{\tau_{\mathrm{sm}}}{\tau_{\mathrm{tr}}}\right), \quad G_0^{\mathrm{mix}}(x,\gamma) = \begin{cases} -\ln x + (2\gamma)^{1/2}, & x \ll 1, \\ 4c_0\gamma^{1/2}x^{-1/2}, & x \gg 1. \end{cases}$$

In the case of Coulomb interaction, the exchange contribution is given by

$$\frac{\delta\rho_{xx}^{\mathrm{F,mix}}(B)}{\rho_0} = -\frac{(\omega_c\tau_{\mathrm{tr}})^2}{\pi k_F l} G_{\mathrm{F}}^{\mathrm{mix}}\left(T\tau_{\mathrm{tr}}, \frac{\tau_{\mathrm{sm}}}{\tau_{\mathrm{tr}}}\right), \quad G_{\mathrm{F}}^{\mathrm{mix}}(x,\gamma) = \begin{cases} -\ln x + (\gamma/2)^{1/2}, & x \ll 1, \\ 2c_0\gamma^{1/2}x^{-1/2}, & x \gg 1. \end{cases}$$

These results (illustrated in Fig. 10) are in a good agreement with experimental data of Ref. [58] for mixed disorder in a Si/SiGe heterostructure. Finally, the ballistic contribution to ρ_{xy} is also enhanced by a factor $\sim (\tau_{\mathrm{sm}}/\tau_{\mathrm{tr}})^{1/2}$ in the mixed disorder model.

The formalism can be further applied to anisotropic systems. The interaction-induced correction mixes the components ρ_{xx} and ρ_{yy} of the resistivity tensor. This result is of special interest in the case of systems subject to a one-dimensional periodic modulation (lateral superlattice, Sec. 3; wave vector $\mathbf{k} \parallel \mathbf{e}_x$). Specifically, it has been shown that the interaction induces novel oscillations in ρ_{yy}, which are in phase with quasiclassical commensurability (Weiss) oscillations in ρ_{xx}.

5 Influence of Landau quantization on magnetotransport

In this section, we address magnetooscillations in the dissipative dc and ac conductivity of a 2DEG governed by the Landau quantization. Despite these effects, to the first place, Shubnikov-de Haas oscillations (SdHO), are well established experimentally, the theoretical description until recently was only available [59] for fully separated Landau levels (LLs) with point-like scatterers [60]. A systematic approach to the problem was developed in Ref. [61]. The results of this work, valid also for overlapping LLs, and for experimentally relevant case of smooth disorder, with the correlation length $d \gg k_F^{-1}$, are reviewed below.

Within the quasiclassical Boltzmann theory, the dissipative *ac* conductivity $\sigma_\omega = \sigma_+(\omega) + \sigma_-(\omega)$ of a non-interacting 2DEG is given by the Drude formula (we neglect spin for simplicity),

$$\sigma_\pm^D(\omega) = (1/4)e^2\nu_0 v_F^2\tau_{\mathrm{tr}}/[1 + (\omega_c \pm \omega)^2\tau_{\mathrm{tr}}^2]\,, \tag{30}$$

where $\nu_0 = m/2\pi$ and τ_{tr} are the density of states (DOS) and the transport relaxation time at $B = 0$, $\omega_c = eB/mc$ the cyclotron frequency, and m is the electron effective mass. We consider a 2DEG subjected to quantizing magnetic field B and a random potential $U(\mathbf{r})$ characterized by a correlation function $\langle U(\mathbf{r})U(\mathbf{r}')\rangle = W(|\mathbf{r} - \mathbf{r}'|)$. The total and the transport relaxation rates at $B = 0$ are

$$\left.\begin{array}{l} \tau_{\mathrm{q}}^{-1} \\ \tau_{\mathrm{tr}}^{-1} \end{array}\right\} = 2\pi\nu_0 \int \frac{d\phi}{2\pi}\, \tilde{W}(2k_F \sin\frac{\phi}{2}) \times \left\{\begin{array}{l} 1 \\ (1-\cos\phi) \end{array}\right. ,$$

where $\tilde{W}(\mathbf{q})$ is the Fourier transform of $W(\mathbf{r})$. While we are mainly interested in the experimentally relevant case of smooth disorder, $d \gg k_F^{-1}$, with $\tau_{\mathrm{tr}}/\tau_{\mathrm{q}} \sim (k_F d)^2 \gg 1$, our results are valid for arbitrary d (i.e., including short-range disorder with $\tau_{\mathrm{tr}}/\tau_{\mathrm{q}} \sim 1$). The conductivity is given by the Kubo formula

$$\sigma_\omega = -(e^2/4\pi V\omega)\int d\varepsilon\,(f_\varepsilon - f_{\varepsilon+\omega})\mathrm{Tr}\,\overline{\hat{v}_x(G^A_{\varepsilon+\omega} - G^R_{\varepsilon+\omega})\hat{v}_x(G^A_\varepsilon - G^R_\varepsilon)}\,, \tag{31}$$

where f_ε is the Fermi distribution, $G^{R,A}$ are the retarded and advanced Green functions, the bar denotes impurity averaging, and V is the system area. At high LLs, $\varepsilon_F \gg \omega, \omega_c$, disorder can be treated within the self-consistent Born approximation (SCBA) [59] provided the disorder correlation length satisfies $d \ll l_B$ and $d \ll v_F\tau_{\mathrm{q}}$, where $l_B = (c/eB)^{1/2}$ is the magnetic length [62]. The SCBA equations for the Green function in the LL representation, $G_n^R = (G_n^A)^*$, read [59, 62],

$$G_n^R(\varepsilon) = (\varepsilon - \varepsilon_n - \Sigma_\varepsilon)^{-1}, \qquad \Sigma_\varepsilon = (\omega_c/2\pi\tau_{q,0})\sum\nolimits_n G_n^R(\varepsilon)\,, \tag{32}$$

where $\varepsilon_n = (n + \frac{1}{2})\omega_c$ is the n-th LL energy (Fig. 12a). The conductivity (31) is given by an electronic bubble with a vertex correction, i.e., by a sum of ladder diagrams, Fig. 12b,c. In the case of white-noise disorder, $\tau_{\rm q} = \tau_{\rm tr}$, the vertex correction is zero, and it suffices to evaluate the bare bubble

$$\sigma^b_\pm(\omega) = \frac{e^2 v_F^2 \nu_0}{4} \int \frac{d\varepsilon}{\omega}\, (f_\varepsilon - f_{\varepsilon+\omega})\, {\rm Re}(\Pi^{RA}_\pm - \Pi^{RR}_\pm), \qquad \Pi^{RR(RA)}_\pm = \frac{\omega_c}{2\pi} \sum_n G^R_{n\pm 1}(\varepsilon+\omega) G^{R(A)}_n(\varepsilon).$$

For the case of smooth disorder we have to take into account the vertex correction (Fig. 1c) while averaging in Eq. (31). This is a non-trivial task since the disorder mixes strongly the LLs, thus seriously complicating a direct calculation in the LL representation. The result, however, acquires a remarkably simple and physically transparent form: provided the above SCBA conditions are fullfilled, the inclusion of the vertex correction results in a replacement of $\Pi^{RR(RA)}_\pm$ above by $\Pi^{RR(RA)}_{\pm,\rm tr} \equiv \left[\left(\Pi^{RR(RA)}_\pm \right)^{-1} - (\tau_{\rm q}^{-1} - \tau_{\rm tr}^{-1}) \right]^{-1}$. It follows that σ_ω has a Drude-type structure with the DOS, $\nu(\varepsilon) = -\pi^{-1}\nu_0\omega_c {\rm Im} \sum_n G^R_n(\varepsilon)$, and the transport time renormalized due to Landau quantization:

$$\sigma_\pm(\omega) = \frac{e^2 v_F^2}{4\omega} \int \frac{d\varepsilon\, (f_\varepsilon - f_{\varepsilon+\omega})\, \nu(\varepsilon)\, \tau^{-1}_{\rm tr,B}(\varepsilon+\omega)}{[\tau^{-2}_{\rm tr,B}(\varepsilon) + \tau^{-2}_{\rm tr,B}(\varepsilon+\omega)]/2 + (\omega \pm \omega_c)^2}\,, \qquad \tau_{\rm tr,B}(\varepsilon) \equiv \tau_{\rm tr} \frac{\nu_0}{\nu(\varepsilon)}\,. \tag{33}$$

Formula (33) is the main result of this section. Let us emphasizethat the single-particle time $\tau_{\rm q}$ enters Eq. (33) only through the DOS; everywhere else it has been replaced by the transport time $\tau_{\rm tr}$ due to the vertex correction. In the following, we analyze Eq. (33) in several important limiting cases.

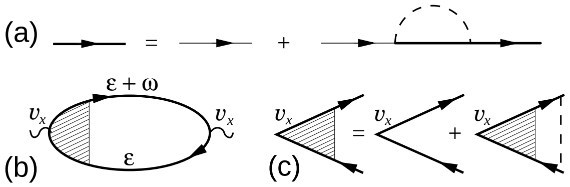

Fig. 12 (a) SCBA equation for the Green function; (b) dynamical conductivity with vertex correction (c).

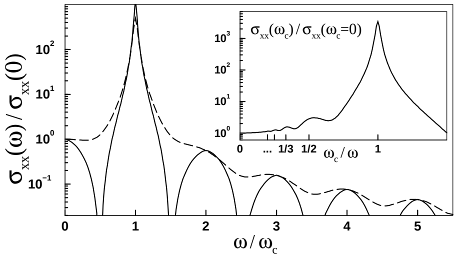

Fig. 13 Magnetooscillations of the dynamical conductivity for $\tau_{\rm tr}/\tau_{\rm q} = 10$. Solid line: separated LLs, $\omega_c\tau_{\rm q}/\pi = 3.25$; dashed line: overlapping LLs, $\omega_c\tau_{\rm q}/\pi = 1$. Inset: σ_{xx} for fixed $\omega\tau_{\rm q}/2\pi = 1$ as a function of ω_c.

In the regime of strongly overlapping LLs, $\omega_c\tau_{\rm q} \ll 1$, the solution to SCBA equations (32) is most easily obtained using the Poisson formula, $\sum_n F_n = \sum_k \int dx F(x) \exp(2\pi i k x)$. The $k = 0$ term yields the $B = 0$ result, while the $k = \pm 1$ contributions provide the leading oscillatory correction to the DOS,

$$\nu(\varepsilon) = \nu_0[1 - 2\delta\cos(2\pi\varepsilon/\omega_c) + \mathcal{O}(\delta^2)]\,, \qquad \delta = \exp(-\pi/\omega_c\tau_{\rm q}) \ll 1\,. \tag{34}$$

To first order in δ, Eq. (33) produces the following result:

$$\frac{\sigma^{(1)}_\pm(\omega)}{\sigma^D_\pm(\omega)} = 1 - 2\delta\, \mathcal{F}\left(\frac{2\pi^2 T}{\omega_c}\right) \cos\frac{2\pi\varepsilon_F}{\omega_c} \left[\frac{2\alpha_\pm^2}{\alpha_\pm^2 + 1} \frac{\sin(2\pi\omega/\omega_c)}{2\pi\omega/\omega_c} + \frac{3\alpha_\pm^2 + 1}{\alpha_\pm^2 + 1} \frac{\sin^2(\pi\omega/\omega_c)}{\alpha_\pm \pi\omega/\omega_c} \right]\,, \tag{35}$$

where $\alpha_\pm \equiv \tau_{\rm tr}(\omega \pm \omega_c)$, and the Dingle factor $\mathcal{F}(X) = X/\sinh X$ describes the T–damping of the SdHO. In the *dc* limit $\omega \to 0$, this result confirms the form of SdHO in smooth disorder conjectured in [63]. If T is higher than the Dingle temperature $T_D \equiv 1/2\pi\tau_{\rm q}$, the temperature smearing becomes the dominant damping factor. In high-mobility 2DEG the Dingle temperature is as low as $T_D \sim 100\,{\rm mK}$, so that for characteristic measurement temperatures $T \sim 1\,\mathrm{K}$ the first-order correction (35) will be completely suppressed. However, there exists a correction of order δ^2, oscillatory in ω/ω_c, which is not affected by the temperature. To obtain it, there is no need to calculate $\nu(\varepsilon)$ to second order, since the corresponding terms oscillate with ε, and doesn't survive the high–T limit. The leading quantum correction at $T \gg T_D$ results from the averaging Eq. (33) over fast energy oscillations of the first-order $\nu(\varepsilon)$, Eq. (34), which gives

$$\sigma_{\pm}^{(2)}(\omega) = \sigma_{\pm}^{D}(\omega) \left\{ 1 + 2\delta^2 \left[\frac{\alpha_{\pm}^2(\alpha_{\pm}^2 - 3)}{(\alpha_{\pm}^2 + 1)^2} \cos\frac{2\pi\omega}{\omega_c} + \frac{\alpha_{\pm}(3\alpha_{\pm}^2 - 1)}{(\alpha_{\pm}^2 + 1)^2} \sin\frac{2\pi\omega}{\omega_c} \right] \right\} . \tag{36}$$

The regime which is most interesting theoretically and relevant experimentally is that of long-range disorder, $\tau_{\mathrm{tr}}/\tau_{\mathrm{q}} \gg 1$, and a classically strong magnetic field, $\omega_c, \omega \gg \tau_{\mathrm{tr}}^{-1}$. In this situation Eq. (33) reads

$$\sigma_{\omega} = \sigma_{\omega}^{D} \int d\varepsilon \frac{f_{\varepsilon} - f_{\varepsilon+\omega}}{\omega\, \nu_0^2}\, \nu(\varepsilon)\, \nu(\varepsilon + \omega) \, , \qquad \sigma_{\omega}^{\mathrm{D}} = \sum_{\pm} \frac{e^2 \nu_0 v_{\mathrm{F}}^2}{4\tau_{\mathrm{tr}}(\omega \pm \omega_c)^2} \, , \tag{37}$$

or, in *dc* limit,

$$\sigma_{\mathrm{dc}} = -\sigma_{\mathrm{dc}}^{D} \int d\varepsilon [\nu^2(\varepsilon)/\nu_0^2] \partial_{\varepsilon} f(\varepsilon) \, , \qquad \sigma_{\mathrm{dc}}^{\mathrm{D}} = e^2 \nu_0 v_{\mathrm{F}}^2 / 2\tau_{\mathrm{tr}} \omega_c^2 \, , \tag{38}$$

In the limit of separated LLs, $\omega_c \tau_{\mathrm{q}} \gg 1$, the DOS is a sequence of semicircles of width $2\Gamma \ll \omega_c$,

$$\nu(\varepsilon) = \nu_0 \tau_{\mathrm{q}} \sum\nolimits_n \mathrm{Re} \sqrt{\Gamma^2 - (\varepsilon - \varepsilon_n)^2} \, , \qquad \Gamma = \sqrt{2\omega_c/\pi\tau_{\mathrm{q}}} \, . \tag{39}$$

In this case, σ_{ω} is non-zero only for ω in intervals $[M\omega_c - 2\Gamma,\ M\omega_c + 2\Gamma]$ with an integer M.

Oscillations in σ_{ω} with ω/ω_c for 2DEG with smooth disorder at $\omega_c \tau_{\mathrm{tr}} \gg 1$ and $T \gg T_D$ are illustrated in Fig. 13. For overlapping LLs, oscillations away from the cyclotron peak are described by simple formula $\sigma_{\omega}/\sigma_{\omega}^{\mathrm{D}} = 1 + 2\delta^2 \cos(2\pi\omega/\omega_c)$. For separated LLs, at the center of the $M = 1$ interval we find a CR peak of height $\sigma_{xx}(\omega = \omega_c) = (e^2 \nu_0 v_F^2 / \pi\Gamma) \tau_{\mathrm{tr},0}/\tau_{\mathrm{q}}$ and width $\sim \Gamma \tau_{\mathrm{q}}/\tau_{\mathrm{tr},0}$. All other peaks ($M \neq 1$) are smaller by a factor $\sim \tau_{\mathrm{tr}}/\tau_{\mathrm{q}} \sim (k_F d)^2 \gg 1$,

$$\sigma_{xx}(\omega = M\omega_c) = (4e^2 \nu_0 v_F^2 \Gamma / 3\pi\omega_c^2)(\tau_{\mathrm{q}}/\tau_{\mathrm{tr}})[(M^2 + 1)/(M^2 - 1)^2] \, . \tag{40}$$

6 Interaction effects in quantizing magnetic fields

6.1 Interaction effects on oscillations

In this Section we discuss the interaction effects on magnetooscillations (de Haas-van Alphen and Shubnikov – de Haas oscillations), closely following Ref. [64]. In addition to experimental motivation related to the apparent metal-insulator transition in two-dimensional systems, the corresponding theory complements the recently developed theory of interaction effects in transport of 2D electrons in zero and non-quantizing magnetic fields [55, 56].

The starting point is the expression for the thermodynamic potential derived in the paper by Luttinger and Ward [65]

$$\Omega = -T \mathrm{Tr} \ln(-G^{-1}) - T \mathrm{Tr}(G\Sigma) + \Omega', \tag{41}$$

where the trace implies summation over Landau levels N and over fermionic Matsubara frequencies $\epsilon_n = (2n + 1) i\pi T$, $G(i\epsilon_n, N\omega_c) = [i\epsilon_n + \mu - (N + 1/2)\omega_c - \Sigma(i\epsilon_n, N\omega_c)]^{-1}$ is the dressed Matsubara Green's function, and $\Sigma(i\epsilon_n, N\omega_c)$ is a self-energy part of Green's function which includes all the disorder and interaction effects. The terms $-T\mathrm{Tr}(G\Sigma)$ and Ω' in (41) are introduced to avoid double-counting of

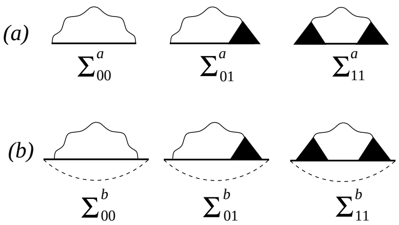

Fig. 14 Self energy diagrams in the first order in the effective interaction (wavy line). Black triangles denote impurity ladders Γ dressing interaction vertices, dashed line is a single-impurity line. Diagrams (b) represent the "Hikami-box" contribution to the self-energy which restores the gauge-invariance of the damping.

diagrams [65, 66]. The term Ω' denotes the sum of all so-called skeleton diagrams with all bare Green's functions replaced by dressed Green's functions.

As shown in Ref. [67], the exponential decay of magnetooscillations is described by the $\mathrm{Tr}\ln$-term. The oscillatory parts of the additional terms, which are introduced to correct for overcounting, cancel each other. In order to obtain the correction to the thermodynamic potential one needs to calculate the self-energy part of the Green's function. It is worth noting that the inelastic contribution to the self-energy $\propto [(\pi T)^2 - \epsilon_n^2]\mathrm{sign}\epsilon_n$ vanishes for $\epsilon_n = \pi T$, and thus does not affect the damping of the magnetooscillations $B(T)$ for $T \gg \omega_c$, in agreement with Refs. [68, 69].

For overlapping Landau levels [Eq. (34)], the magnetooscillations are damped by disorder even at zero temperature via the standard Dingle factor $\delta = \exp(-\pi/\omega_c\tau_q)$. Therefore we will consider only the first harmonics of the oscillations, A_1, neglecting all higher harmonics whose damping is much stronger. In what follows we concentrate on the case $T \gg \omega_c$. Under this condition, the first harmonics of the oscillatory part of the thermodynamic potential

$$\Omega_{\mathrm{osc}} \simeq 2\nu_0\,(\omega_c/2\pi)^2\,A_1\cos(2\pi^2 n_e/eB), \tag{42}$$

is given by

$$A_1 = (4\pi^2 T/\omega_c)\,\exp\left[-2\pi^2 T/\omega_c^* - \pi/\omega_c^*\tau_q^*\right]\,\exp[B(T)], \tag{43}$$

which is a standard FL Lifshitz-Kosevich expression multiplied by the additional factor with

$$B(T) = -2\pi i\,Z\,\delta\Sigma(i\pi T, \xi_0)/\omega_c^*. \tag{44}$$

Here $\omega_c^* = eB/m^*$ is the Fermi-liquid (FL) renormalized effective cyclotron frequency in a pure system at zero T, which is related to the FL-renormalized effective mass m^*, Z is the FL Z-factor (given by the residue of the Green's function), τ_q^* is the FL-renormalized scattering time, and $\delta\Sigma(i\epsilon_n, \xi_0)$ is the self-energy part (taken at the pole ξ_0 of the Green's function in the presence of disorder) describing the interplay of disorder and interaction.

Hereafter white-noise disorder with $\tau_{\mathrm{tr}} = \tau_q \equiv \tau$ is considered. Evaluating the sum of six digrams (Fig. 14) for $\delta\Sigma$, one gets the following expression for the damping exponent in the case of short-range interaction U_0:

$$B(T) = -\mathrm{const}\,\nu_0 U_0(\pi/\omega_c\tau_q) + (\pi T/\omega_c)\,(\nu_0 U_0/\varepsilon_F\tau)\ln(\varepsilon_F/T). \tag{45}$$

The first term in Eq. (45) describes the T-independent FL-renormalization of τ_q due to vertex corrections and should be included in the effective relaxation time τ_q^*. The second term represents the T-dependent contribution to the damping factor that we are interested in and is analyzed below.

The above result (45) can be interpreted in terms of corrections to the effective mass (or ω_c) and the quantum elastic scattering rate τ_q entering the standard Lifshitz-Kosevich formula. These corrections come from the interplay of disorder and interaction, leading to

$$B(T) = -(2\pi^2 T/\omega_c)(\delta m/m) - (\pi/\omega_c\tau_q)\left[\delta m/m - \delta\tau_q/\tau_q\right]. \tag{46}$$

It is worth noting that the FL-renormalization does not affect the product $\omega_c m = eB$.

Comparing (45) and (46), one can see that the $T \ln T$ dependence of the damping factor could in principle originate either from the $\ln T$ correction to the effective mass, or from the $T \ln T$-type correction to τ_q. This led the authors of Ref. [68] to the conclusion that the nonlinear $T-$dependence of the damping factor may be equivalently interpreted either as a $T-$dependent renormalization of the effective mass or as a $T-$dependent Dingle temperature. It is clear, however, that these two possibilities correspond to different physical processes. To identify the physical origin of the leading contribution to the damping it is instructive to obtain $B(T)$ using the expression for the self-energy analytically continued to real values of energies $\epsilon_n \to -i\varepsilon$.

Having calculated $\mathrm{Re}\Sigma$ and $\mathrm{Im}\Sigma$ for real energies ε, one can determine δm and $\delta\tau_q$. Indeed, the magnitude of the first harmonics of the magnetooscillations of the thermodynamic density of states is expressed through the real-ε self-energy $\delta\Sigma(\varepsilon)$ as follows:

$$A_1(T) = -\int d\varepsilon A_1(\varepsilon, T)\partial_\varepsilon f_T(\varepsilon), \tag{47}$$

$$A_1(\varepsilon, T) = \exp\left\{\frac{2\pi i}{\omega_c}[\varepsilon - \mathrm{Re}\delta\Sigma(\varepsilon, \xi_0)]\right\} \exp\left\{-\frac{\pi}{\omega_c\tau_q} + \frac{2\pi}{\omega_c}\mathrm{Im}\delta\Sigma(\varepsilon, \xi_0)\right\} \tag{48}$$

$$= \exp\left\{\frac{2\pi i\varepsilon}{\omega_c}\left[1 + \frac{\delta m(\varepsilon, T)}{m}\right]\right\} \exp\left\{-\frac{\pi}{\omega_c\tau_q}\left[1 + \frac{\delta m(\varepsilon, T)}{m} - \frac{\delta\tau_q(\varepsilon, T)}{\tau_q}\right]\right\}. \tag{49}$$

where $f_T(\varepsilon) = [1 + \exp(\varepsilon/T)]^{-1}$ is the Fermi distribution function. This allows one to express $\delta\tau_q(\varepsilon, T)$ and $\delta m(\varepsilon, T)$ through $\mathrm{Re}\Sigma(\varepsilon)$ and $\mathrm{Im}\Sigma(\varepsilon)$ as follows:

$$\delta m(\varepsilon, T)/m = -\varepsilon^{-1}\mathrm{Re}\delta\Sigma(\varepsilon, T) = -(\nu_0 U_0/2\pi\varepsilon_F\tau)\ln\{\varepsilon_F/\max[|\varepsilon|, T]\}, \tag{50}$$

$$\begin{aligned}\delta\tau_q(\varepsilon, T)/\tau_q &= 2\tau_q\mathrm{Im}\delta\Sigma(\varepsilon, T) + \delta m(\varepsilon, T)/m \\ &= \nu_0 U_0\frac{T}{\varepsilon_F}\ln\left[2\cosh\left(\frac{\varepsilon}{2T}\right)\right] - \frac{\nu_0 U_0}{2\pi\varepsilon_F\tau}\ln\frac{\varepsilon_F}{\max[|\varepsilon|, T]}.\end{aligned} \tag{51}$$

It is clear from these results that the leading term in $B(T)$ [proportional to $T\ln(\varepsilon_F/T)$, Eq. (45)] originates from the real part of the self-energy, i.e. from renormalization of the effective mass, which affects incommensurability of the oscillations at different values of energy ε. The contribution of the imaginary part of the self-energy, which is governed in the ballistic regime by the renormalization of the scattering time, is smaller by a factor $\ln(\varepsilon_F\tau)$. The obtained result for the interaction-induced correction to the quantum scattering time τ_q, Eq. (51), agrees, up to a factor $\frac{1}{2}$, with the correction to the transport time following from the calculation of conductivity correction in the ballistic regime in Ref. [55].

In the case of Coulomb interaction, one should take into account the dynamical screening of the interaction within the random phase approximation (RPA). This leads to different asymptotics of the self-energy in the diffusive and ballistic regimes, in contrast to the case of weak short-range interaction. The T-dependence of the leading correction to the magnetooscillations damping factor due to the interaction in the singlet channel has the form (Fig. 15)

$$B^\rho(T) = \frac{\pi}{\omega_c\tau_q}\frac{T}{\varepsilon_F} \times \begin{cases} (3/2)\ln(\varepsilon_F/T) - (1/2)\ln(4\pi\varepsilon_F\tau), & 4\pi T\tau \ll 1, \\ \\ \ln(\varepsilon_F/T), & 4\pi T\tau \gg 1. \end{cases} \tag{52}$$

Calculation of the corresponding triplet contribution leads to qualitatively similar asymptotics. The leading term in the total correction to the damping factor in the ballistic regime, realized in experiments on low-disorder samples at realistic temperatures, takes the simple form

$$B(T) = B^\rho(T) + B^\sigma(T) \simeq [1 + 3F_0^\sigma(1 + F_0^\sigma)^{-1}]\,(\pi T/\omega_c\tau_q\varepsilon_F)\,\ln(\varepsilon_F/T). \tag{53}$$

As discussed above, this result arises due to the correction to the effective mass.

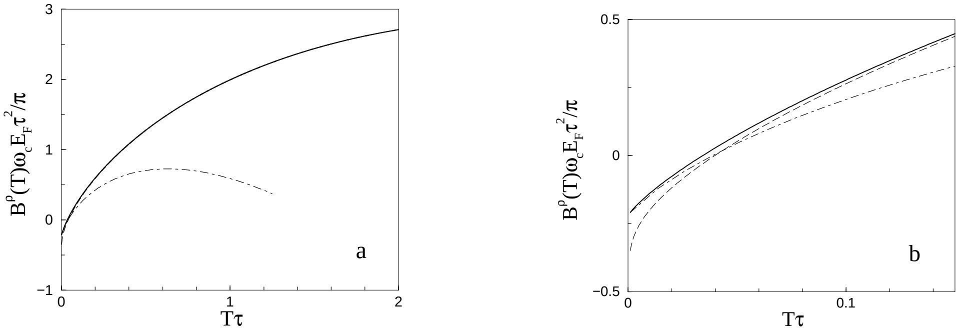

Fig. 15 Temperature dependence of the singlet channel correction to the damping factor $B^\rho(T)$ for $4\pi\varepsilon_F\tau = 100$ (solid line) with the low-T (dot-dashed) and high-T (dashed) asymptotics. (a) Wide temperature range: on this scale $B^\rho(T)$ is essentially indistinguishable from its high-T asymptotics; (b) low-T part: the crossover between the two asymptotics occurs at $T\tau \sim 0.05$.

6.2 Coulomb drag in high Landau levels

Coulomb drag between parallel two-dimensional electron systems [70, 71] has developed into a powerful probe of quantum-Hall systems [72, 73, 74, 75, 76, 77, 78, 79], providing information which is complementary to conventional transport measurements. The drag signal is the voltage V developing in the open-circuit passive layer when a current I is applied in the active layer. The drag resistance (also known as transresistance) is then defined by $R_D = V/I$. As a function of interlayer spacing a, the interlayer coupling changes from weak at large spacings where it can be treated in perturbation theory, to strong at small spacings where it can result in states with strong interlayer correlations [76, 77].

In a simple picture of Coulomb drag, the carriers of the active layer transfer momentum to the carriers of the passive layer by interlayer electron-electron scattering. The phase space for interlayer scattering is proportional to the temperature T in either layer predicting a monotonous temperature dependence $R_D \propto T^2$ of the drag resistance. Moreover, the signs of the voltages in active and passive layer are expected to be opposite (the same) for carriers of equal (opposite) charge in the two layers [80].

Remarkably, experiments show that Coulomb drag behaves very differently from these simple expectations when a perpendicular magnetic field B is applied such that the Fermi energy ε_F is in a high Landau level, $\varepsilon_F/\hbar\omega_c \gg 1$. ($\omega_c$ is the cyclotron frequency.) Several experiments [74, 78] in the regime of weak interlayer coupling observed negative drag when the filling factors in the two layers are different. A more recent experiment [79] also reveals a non-monotonic dependence on temperature. While the drag resistivity shows a quadratic temperature dependence at sufficiently high temperatures, where drag is always positive, an additional peak develops at low temperatures which can have both a positive or a negative sign depending on the filling-factor difference between the two layers.

In this Section, we present the theory of Coulomb drag in the limit of high Landau levels [82]. In a strong magnetic field, $\omega_c\tau_{\text{tr}} \gg 1$, the intralayer Hall resistivity ρ_{xy} dominates over the longitudinal resistivity ρ_{xx}. Therefore, the drag resistivity is given by

$$\rho^D_{xx} \simeq \rho^{(1)}_{xy}\, \sigma^D_{yy}\, \rho^{(2)}_{yx} \tag{54}$$

The Coulomb drag in strong magnetic fields is an interplay of two contributions, as illustrated in Fig. 16. At high temperatures, the leading contribution is due to breaking of particle-hole symmetry by the curvature of the zero-B electron spectrum. This "normal" contribution to the drag is always positive and increases in a broad temperature range as T^2. At low temperatures, another, "anomalous", contribution dominates, which arises from the breaking of particle-hole symmetry by the energy dependence of the density of states related to Landau quantization. This contribution is sharply peaked at a temperatute $T \sim \Delta$ (where

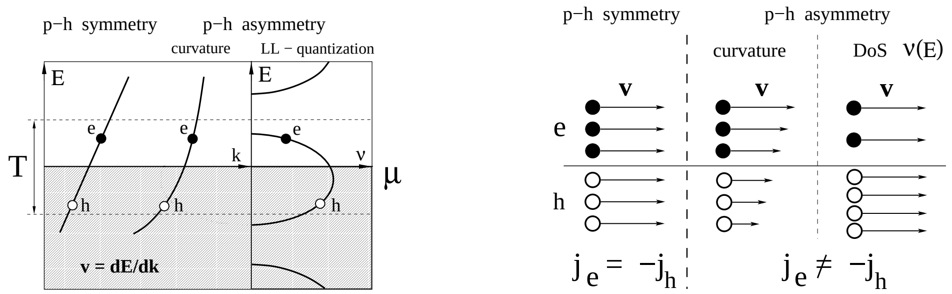

Fig. 16 Schematic illustration of different sources of particle-hole asymmetry: curvature of zero-B spectrum $E(k)$ vs LL-quantization of the density of states (DoS) $\nu(E)$. In the particle-hole (p-h) symmetric case, the electronic and hole contributions to the current induced in the passive layer (j_e and j_h, respectively) compensate each other. When the p-h asymmetry is generated by a finite curvature, the velocities of electrons and holes (shown by arrows in the right panel) are different, which destroys the compensation. This is the "conventional" mechanism of the drag. When the DoS depends on energy (in the present case because of the LL-quantization), an "anomalous" drag arises due to the difference in numbers of occupied electronic and hole states.

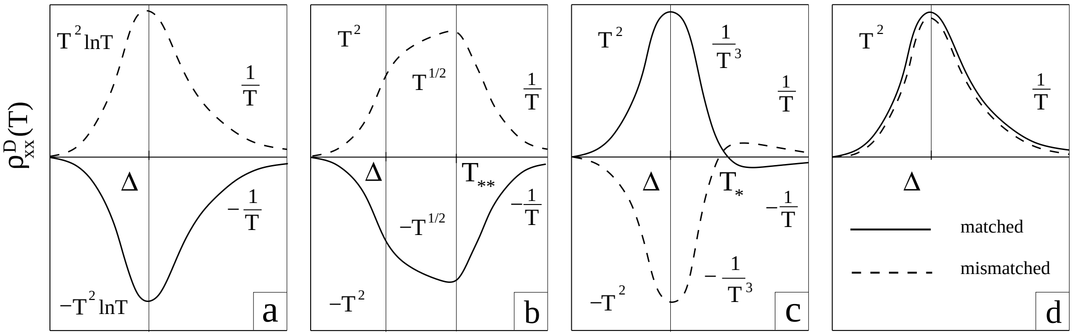

Fig. 17 Schematic temperature dependence of low-temperature drag in different regimes: a) diffusive, $R_c/a \ll 1$; b) weakly ballistic, $1 \ll R_c/a \ll \omega_c/\Delta$; c) ballistic, $\omega_c/\Delta \ll R_c/a \ll N\Delta/\omega_c$; d) ultra-ballistic, $N\Delta/\omega_c \ll R_c/a$.

$\Delta = 2\Gamma$ is the Landau level width) and has an oscillatory sign depending on the density mismatch between the two layers.

Since the momenta transferred from one layer to the other are effectively restricted by the inverse interlayer distance, a^{-1}, the behavior of the transresistivity will be essentially dependent on the relation between R_c and a. Specifically, with increasing R_c/a the following four regimes are identified i) diffusive, $R_c/a \ll 1$, ii) weakly ballistic, $1 \ll R_c/a \ll \omega_c/\Delta$, iii) ballistic, $\omega_c/\Delta \ll R_c/a \ll N\Delta/\omega_c$, and iv) ultra-ballistic, $N\Delta/\omega_c \ll R_c/a$. In all regimes, the temperature-dependence of the drag resistivity is non-monotonous: the absolute value of $\rho^D_{xx}(T)$ shows a peak around $T \sim \Delta$ and increases again at $T \gg \omega_c$. However, the $T-$ and $B-$ dependences of ρ^D_{xx}, as well as the sign of the low-temperature peak (the high-temperature drag is always positive), are specific for each particular regime, as illustrated in Fig. 17 and summarized below.

Diffusive regime, $R_c/a \ll 1$. In the diffusive regime, the drag at not too high temperatures, $T \ll \omega_c$, is governed by the diffusive rectification[81] which can be calculated quasiclassically using the local approximation for the density dependence of the conductivity. As a result, the sign of the drag at $T \sim \Delta$ oscillates but is opposite to what we found above for the ballistic regime: the drag is negative for equal densities.[81] At the “slopes” of the peak, ρ_{xx}^D scales with T and B in the following way

$$\rho_{xx}^D \propto \begin{cases} -\,T^2\ \ln(TB^{3/2}), & T \ll \Delta, \\ -\,T^{-1}B^{3/2}\ \ln B, & T \gg \Delta, \end{cases} \tag{55}$$

where the sign corresponds to the case of matching densities.

Weakly ballistic regime, $1 \ll R_c/a \ll \omega_c/\Delta$. This regime is qualitatively similar to the diffusive regime with

$$\rho_{xx}^D \propto \begin{cases} -\,T^2\ B^{-5/4}, & T \ll \Delta, \\ -\,T^{1/2}\ B^{-1/2}, & \Delta \ll T \ll T_{**} \equiv \omega_c(a/R_c) \\ -\,T^{-1}\ B^{5/2}, & T \gg \omega_c(a/R_c), \end{cases} \tag{56}$$

The sign of the peak oscillates just like in the diffusive regime.

Ballistic regime, $\omega_c/\Delta \ll R_c/a \ll N\Delta/\omega_c$. The *ballistic* regime is most relevant experimentally. In this regime, the drag is governed by the particle-hole asymmetric effect of Landau quantization of the density of states and the sign of the drag oscillates,

$$\rho_{xx}^D \propto \begin{cases} T^2\ B\ \ln(B_*/B), & T \ll \Delta, \\ T^{-3}\ B^{7/2}\ \ln(B_*/B), & \Delta \ll T \ll T_* \equiv \Delta \ln^{1/2}(R_c\Delta/a\omega_c), \\ -\,T^{-1}\ B^{5/2}, & T \gg T_*, \end{cases} \tag{57}$$

where $B_* \sim (mc/e)(v_F^2/a^2\tau_0)^{1/3}$ (experimentally, the logarithmic factor in T_* is typically of the order of unity, so that the intermediate regime may not be fully developed). We emphasize that the drag at low temperatures is positive for matched and negative for mismatched densities.

Ultra-ballistic regime, $N\Delta/\omega_c \ll R_c/a$. The drag for all temperatures is determined by the conventional contribution related to the curvature of the electron dispersion and is always positive,

$$\rho_{xx}^D \propto \begin{cases} T^2\ B^2, & T \ll \Delta, \\ T^{-1}\ B^{7/2}, & T \gg \Delta, \end{cases} \tag{58}$$

At high temperature, $T \gg \omega_c$, the drag is governed by the conventional contribution (and is therefore positive) in all the regimes. It is linear in T in the diffusive regime ($\rho_{xx}^D \propto TB^{-1/2}$). In all the ballistic regimes the drag resistivity scales as $\rho_{xx}^D \propto T^2B^{1/2}$ for $\omega_c \ll T \ll v_F/a$ and $\rho_{xx}^D \propto TB^{1/2}$ for $T \gg v_F/a$.

A comparison of Fig. 18 with Fig. 3 of Ref. [79] reveals a remarkable agreement between the experimental findings and the theoretical results. In both the theory and the experiment, (i) $\rho_{xx}^D(T)$ shows a sharp peak at low temperatures; (ii) the sign of the drag in this temperature range oscillates as a function of the filling factor of one layer (at fixed filling factor of the other layer); (iii) the low-T drag is positive for equal filling factors and negative when the Fermi energy in one layer is in the upper half and in the other layer in the lower half of the Landau band; (iv) the high-T drag is always positive, independently of the difference in filling factors of two layers and increases monotonically with increasing T. Furthermore, it was observed by Muraki *et al* that in the low-temperature regime of initial increase of ρ_{xx}^D, as well as in the high-temperature regime of “normal” drag, the drag resistivity can be described by an empirical scaling law, $\rho_{xx}^D \propto (n/B)^{-2.7}f(T/B)$. Theoretical results for both the low- and high-temperature regimes are in a nice correspondence with this prediction, with $f(x) \sim x^2$.

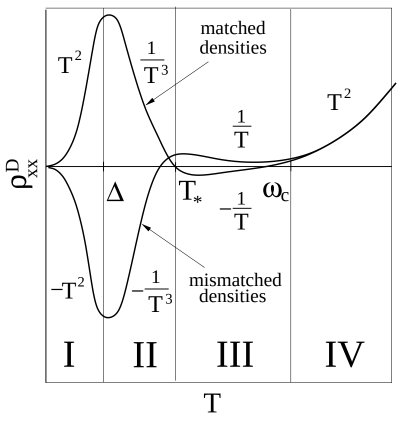

Fig. 18 Schematic temperature dependence of drag in the ballistic regime for matched and mismatched densities. In the latter case the mismatch is chosen such that the drag is negative at low T (see text). Scaling of ρ^D_{xx} with temperature in different regions is indicated: $T \ll \Delta$ (I); $\Delta \ll T \ll T_*$ (II); $T_* \ll T \ll \omega_c$ (III), and $T \gg \omega_c$ (IV).

7 Photoconductivity

7.1 Microwave-induced magnetoresistance oscillations and zero-resistance states

Recently, a number of new remarkable effects, important for both basic and applied physics, have been discovered in two-dimensional electron systems driven out of equilibrium by strong AC and DC fields. It was observed [83] that dc resistivity ρ_{xx} of a high-mobility 2DEG subjected to microwave radiation of frequency ω exhibits magnetooscillations with a period in ω set by the resonances with multiples of the cyclotron frequency ω_c. Subsequent work on samples with an exceptionally high mobility has shown [84, 85] that for a sufficiently high radiation power the minima of these microwave-induced resistance oscillations (MIRO) evolve into "zero resistance states"(ZRS), in which the dissipative resistance of a sample becomes vanishingly small. Unlike oscillatory ρ_{xx}, the Hall resistivity ρ_{xy} remained practically linear in ω_c. A hallmark of these experimental findings is that the prominent oscillations of the photoconductivity $\sigma_{\rm ph} \simeq \rho_{xx}/\rho_{xy}^2$ are observed at magnetic fields as low as $10\,$mT, and at relatively high temperatures up to $\sim 1\,$K, at which the Shubnikov-de Haas oscillations are completely suppressed.

Presenting a novel class of magnetooscillations which lead, with increasing ω_c, to apparently dissipationless transport, the experimental results [83, 84, 85] have attracted much theoretical interest. In particular, an explanation of the MIRO has been proposed [86] in terms of a combined effect of radiation and Landau quantization on elementary scattering acts for electrons colliding with impurities (in fact, a closely related theory was put forward long ago [87]). A systematic theoretical study of this mechanism of the MIRO (referred to as a "displacement" mechanism in what follows) was carried out in [88].

On the other hand, it was emphasized [89] that whenever the linear dc response theory predicts a negative resistivity, this signifies an instability leading to the formation of domains of counter-flowing currents. The break-up of an ac-driven sample in current domains provides an explanation to the experimentally observed ZRS.

A different mechanism of the MIRO, called here the "inelastic" mechanism, was proposed in [61] and studied in more detail in [90, 91] (similar ideas were also discussed in [92]). The inelastic mechanism is associated with a radiation-induced non-equilibrium part of the distribution function of electrons $f(\varepsilon)$ which oscillates with varying $\varepsilon \pm \hbar\omega$ due to the Landau quantization. This mechanism yields the amplitude of oscillations of the linear (with respect to the dc field) photoconductivity which is proportional to inelastic scattering time $\tau_{\rm in}$. The inelastic contribution dominates over the displacement one for $\tau_{\rm in}$ larger than single-particle relaxation time τ_q, the condition which is fulfilled in the experiments. Apart from the magnitude of the effect, the two contributions are qualitatively different in their dependence on T and polarization of the radiation. In accord with the experiments, the inelastic contribution decreases as $\tau_{\rm in} \propto T^{-2}$ with increasing T and does not depend on the direction of linear polarization of the microwave field. By contrast, the displacement mechanism [86, 87, 88] yields a T independent contribution which depends essentially on the relative orientation of the microwave and dc fields, which clearly contradicts the experimental findings.

7.2 Inelastic mechanism of MIRO

We consider a high-mobility 2DEG, with $\tau_{\rm q} \ll \tau_{\rm tr}$, subjected to a classically strong transverse magnetic field, $\omega_c\tau_{\rm tr} \gg 1$ (we use notations of Sec. 5, in particular, $\tau_{\rm q}$ and $\tau_{\rm tr}$ are specified in Eq. (31). The photoconductivity $\sigma_{\rm ph}$ determines the longitudinal current flowing in response to a *dc* electric field $\mathcal{E}_{\rm dc}$, $\vec{j}\cdot\vec{\mathcal{E}}_{\rm dc} = \sigma_{\rm ph}\mathcal{E}_{\rm dc}^2$, in the presence of a microwave electric field $\mathcal{E}_\omega \cos\omega t$. The more frequently measured [83, 84, 85, 92] longitudinal resistivity, $\rho_{\rm ph}$, is given by $\rho_{\rm ph} \simeq \rho_{xy}^2\sigma_{\rm ph}$, where $\rho_{xy} \simeq eB/n_e c$ is the Hall resistivity, affected only weakly by the radiation.

Here we study the leading inelastic mechanism of MIRO thus taking into account only effects that are due to a non-trivial energy dependence of the non-equlibirum distribution function $f(\varepsilon)$. Photoconductivity $\sigma_{\rm ph}$ is given by the dc responce in the state with non-equlibirum $f(\varepsilon)$. According to Eq. (38),

$$\sigma_{\rm ph} = -\sigma_{\rm dc}^D \int d\varepsilon\, \tilde{\nu}^2(\varepsilon)\, \partial_\varepsilon f(\varepsilon), \tag{59}$$

where $\tilde{\nu}(\varepsilon) = \nu(\varepsilon)/\nu_0$. The non-equlibirum distribution function $f(\varepsilon)$ is found as a solution of the stationary kinetic equation

$$\mathcal{E}_\omega^2\, \frac{\sigma_\omega^{\rm D}}{2\omega^2\nu_0} \sum_\pm \tilde{\nu}(\varepsilon\pm\omega)\, [\, f(\varepsilon\pm\omega) - f(\varepsilon)\,] + \mathcal{E}_{\rm dc}^2\, \frac{\sigma_{\rm dc}^{\rm D}}{\nu_0\tilde{\nu}(\varepsilon)}\, \frac{\partial}{\partial\varepsilon}\left[\tilde{\nu}^2(\varepsilon)\frac{\partial}{\partial\varepsilon} f(\varepsilon)\right] = \frac{f(\varepsilon) - f_T(\varepsilon)}{\tau_{\rm in}}. \tag{60}$$

On the right-hand side of Eq. (60), inelastic processes are included in the relaxation time approximation (which is proven [91] to be sufficient under experimental conditions), and $f_T(\varepsilon)$ is the Fermi distribution. The left-hand side is due to the electron collisions with impurities in the presence of the external electric fields. The first term describes the absorption and emission of microwave quanta; the rate of these transitions is proportional [61] to $\tau_{\rm tr,B}^{-1}(\varepsilon\pm\omega) \propto \nu(\varepsilon\pm\omega)$, see Eqs. (33) and (37). This term can be also extracted from the kinetic equation of Ref. [88]. The second term describes the effect of the *dc* field and can be obtained from the first one by taking the limit $\omega \to 0$. Equation (60) suggests convenient dimensionless units for the strength of the *ac* and *dc* fields:

$$\mathcal{P}_\omega = \frac{\tau_{\rm in}}{\tau_{\rm tr}} \left(\frac{e\mathcal{E}_\omega v_F}{\omega}\right)^2 \frac{\omega_c^2 + \omega^2}{(\omega^2 - \omega_c^2)^2}\,, \qquad \mathcal{Q}_{\rm dc} = \frac{2\,\tau_{\rm in}}{\tau_{\rm tr}} \left(\frac{e\mathcal{E}_{\rm dc} v_F}{\omega_c}\right)^2 \left(\frac{\pi}{\omega_c}\right)^2 . \tag{61}$$

Note that $\mathcal{P}_\omega$ and $\mathcal{Q}_{\rm dc}$ are proportional to $\tau_{\rm in}$ and are infinite in the absence of inelastic relaxation processes.

To first order in $\mathcal{P}_\omega$ and $\mathcal{Q}_{\rm dc} \to 0$, Eq. (60) produces a non-equilibrium correction to $f_T(\varepsilon)$, $f(\varepsilon) - f_T(\varepsilon) = 0.25\mathcal{P}_\omega \sum_\pm \tilde{\nu}(\varepsilon \pm \omega)\, [\, f_T(\varepsilon \pm \omega) - f_T(\varepsilon)\,]$, which oscillates both with ε/ω_c and ω/ω_c due to ε/ω_c–oscillations in the DOS. In turn, the oscillatory $f(\varepsilon)$ leads to ω/ω_c-oscillations of $\sigma_{\rm ph}$, Eq. (59),

$$\sigma_{\rm ph}/\sigma_{\rm dc}^D = \langle\, \tilde{\nu}^2(\varepsilon)\,\rangle_\varepsilon + (\omega\mathcal{P}_\omega/4)\, \langle\, \tilde{\nu}^2(\varepsilon)\, \partial_\varepsilon[\, \tilde{\nu}(\varepsilon+\omega) - \tilde{\nu}(\varepsilon-\omega)\,]\,\rangle_\varepsilon \tag{62}$$

Here we took into account that the SdHO in the experiments are suppressed by temperature, $T \gg T_D$, so that, analogous to Eq. (36), the energy integration results in averaging over ε within the period ω_c, denoted by the angular brackets. For separated LLs, $\omega_c\tau_{\rm q} \gg 1$, with the semielliptical DOS (39), Eq. (62) gives

$$\sigma_{\rm ph}/\sigma_{\rm dc}^{\rm D} = (16\omega_c/3\pi^2\Gamma)\left\{1 - \mathcal{P}_\omega(\omega\omega_c/\Gamma^2)\left[\textstyle\sum_n \Phi\left(\omega/\Gamma - n\omega_c/\Gamma\right) + O\left(\omega_c\mathcal{P}_\omega/\Gamma\right)\right]\right\}, \tag{63}$$

$$4\pi\, \Phi(x) = x\, {\rm Re}[\, 3\arccos(|x| - 1) - (1 + |x|)\sqrt{|x|(2 - |x|)}\,].$$

In the limit of overlapping LLs, the DOS is given by $\tilde{\nu} = 1 - 2\delta\cos\frac{2\pi\varepsilon}{\omega_c}$ with $\delta = \exp(-\pi/\omega_c\tau_{\rm q}) \ll 1$. The existence of a small parameter δ allows one to calculate $\sigma_{\rm ph}$ to all orders in $\mathcal{P}_\omega$ and $\mathcal{Q}_{\rm dc}$,

$$\frac{\sigma_{\rm ph}}{\sigma_{\rm dc}^{\rm D}} = 1 + 2\delta^2\left[1 - \frac{\mathcal{P}_\omega \frac{2\pi\omega}{\omega_c}\sin\frac{2\pi\omega}{\omega_c} + 4\mathcal{Q}_{\rm dc}}{1 + \mathcal{P}_\omega\sin^2\frac{\pi\omega}{\omega_c} + \mathcal{Q}_{\rm dc}}\right]. \tag{64}$$

Results (64) and (63) are shown in Figs. 19 and 20 for several values of $\mathcal{P}_\omega^{(0)} \equiv \mathcal{P}_\omega|_{\omega_c=0}$.

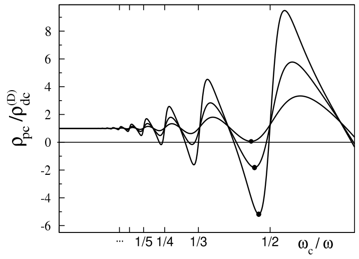

Fig. 19 Photoresistivity (normalized to the Drude value) for overlapping LLs vs ω_c/ω at fixed $\omega\tau_{\rm q} = 2\pi$, and for different $\mathcal{P}_\omega^{(0)} = \{0.24,\ 0.8,\ 2.4\}$. $I-V$ characteristics at the marked minima are shown in Fig. 21.

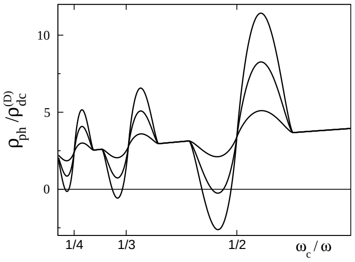

Fig. 20 Photoresistivity (normalized to the Drude value) for separated Landau levels vs ω_c/ω at fixed $\omega\tau_{\rm q} = 16\pi$. The curves correspond to different levels of microwave power $\mathcal{P}_\omega^{(0)} = \{0.01,\ 0.03,\ 0.05\}$.

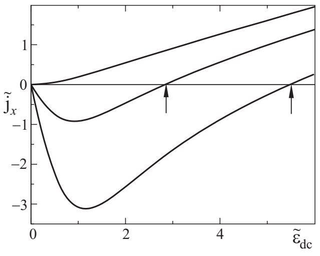

Fig. 21 Current–voltage characteristics [dimensionless current $\tilde{j}_x = (\sigma_{\rm ph}/\sigma_{\rm dc}^{\rm D})\tilde{\mathcal{E}}_{\rm dc}$ vs dimensionless field $\tilde{\mathcal{E}}_{\rm dc} = \mathcal{Q}_{\rm dc}^{1/2}$] at the points of minima marked by the circles in Fig. 19. The arrows show the *dc* field $\tilde{\mathcal{E}}_{\rm dc}^*$ in spontaneously formed domains.

7.3 Zero-resistance states, strong-field domains, oscillatory compressibility

At $\mathcal{P}_\omega$ exceeding certain threshold value $\mathcal{P}_\omega^\star$, $\sigma_{\rm ph}$ around minima becomes negative (see Figs. 19 and 20). According to Ref. [89], this signifies an instability leading to the formation of domains with strong Hall field $\mathcal{E}_{\rm dc} = \pm\mathcal{E}_{\rm dc}^\star$ and counter-flowing currents. The value $\mathcal{E}_{\rm dc}^\star$ is determined by the equation $\sigma_{\rm ph}(\mathcal{P}_\omega, \mathcal{E}_{\rm dc}^\star) = 0$, which in the case of overlapping LLs, Eq. (64), has the solution (marked by arrows in Fig. 21)

$$\mathcal{E}_{\rm dc}^* = \frac{1}{\sqrt{2}\,\pi}\,\frac{\omega_c^2}{ev_F}\left(\frac{\tau_{\rm tr}}{\tau_{\rm in}}\right)^{1/2}\left[\frac{\mathcal{P}_\omega}{\mathcal{P}_\omega^*}-1\right]^{1/2}, \qquad \mathcal{P}_\omega^* = \left(4\delta^2\frac{\pi\omega}{\omega_c}\sin\frac{2\pi\omega}{\omega_c} - \sin^2\frac{\pi\omega}{\omega_c}\right)^{-1}. \quad (65)$$

Equation (65) relates the electric field formed in the domains (measurable by local voltage probe [93]) with the excess power of microwave radiation.

In the case of separated LLs, it suffices to keep the linear-in-$\mathcal{P}_\omega$ term only even for the microwave power $\mathcal{P}_\omega > \mathcal{P}_\omega^* \sim \Gamma^2/\omega\omega_c$ at which the linear-response resistance becomes negative: The second order correction at $\mathcal{P}_\omega \sim \mathcal{P}_\omega^*$ is still small, $\omega_c\mathcal{P}_\omega^*/\Gamma \sim \Gamma/\omega \ll 1$. The strength of the field in domains is determined by the scale at which inter-LL elastic scattering becomes efficient, $\mathcal{E}_{\rm dc}^* \sim (\omega_c^2/ev_F)\sqrt{\tau_{\rm tr}/\tau_{\rm q}}$.

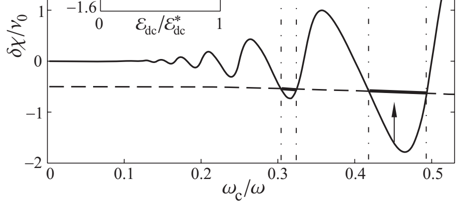

Fig. 22 The microwave-induced correction to the compressibility (solid line) of a 2DEG as a function of ω_c/ω at fixed $\omega\tau_{\rm q} = 2\pi$ and microwave power $\mathcal{P}|_{\omega_c=0} = 1$. In the zero resistance state (ZRS), the electric field inside domains $\mathcal{E}_{\rm dc}^*$ fixes the compressibility at the level shown by a dashed line. Inside the domain wall, the electric field $\mathcal{E}_{\rm dc}$ is smaller than $\mathcal{E}_{\rm dc}^*$ and the compressibility depends on the local field as shown in the inset (for $\omega_c/\omega = 0.45$, this ratio is indicated by the arrow.

In Ref. [94] it was shown that the local compressibility of an irradiated 2DEG, $\chi = \nu_0 + \delta\chi$, exhibits oscillations similar to the MIRO (see Fig. 22). Calculation using Eqs. (60) and (34) yields

$$\delta\chi/\nu_0 = \int d\varepsilon\, \tilde{\nu}(\varepsilon)\partial_\varepsilon[f_T(\varepsilon) - f(\varepsilon)] = -\delta^2 \frac{\mathcal{P}_\omega \frac{2\pi\omega}{\omega_c}\sin\frac{2\pi\omega}{\omega_c} + 4\mathcal{Q}_{\rm dc}}{1 + \mathcal{P}_\omega \sin^2\frac{\pi\omega}{\omega_c} + \mathcal{Q}_{\rm dc}}. \tag{66}$$

The key features of the effect are: (i) the period and the phase of the ω/ω_c-oscillations in χ are the same as in $\sigma_{\rm ph}$, Eq. (64); (ii) the amplitude of the oscillations in χ and $\sigma_{\rm ph}$ have the same dependence on the electron temperature and microwave power; (iii) the ZRS corresponds to a plateau in the compressibility: inside the domains $\chi = \nu_0(1-2\delta^2)/2$. Local measurements of the compressibility may provide a real space snapshot of the domain structure in the ZRS. Experimental work in this direction is currently underway.

7.4 High-power effects, subleading mechanisms, fractional MIRO

In addition to the peak-valley structure near integer ω/ω_c (integer MIRO), several experiments [83, 85, 92, 95, 96, 97, 98] reported similar features near certain fractional values, $\omega/\omega_c = 1/2,\, 3/2,\, 5/2,\, 2/3$.. ("fractional MIRO", or FMIRO), which at elevated microwave power also evolved into ZRS ("fractional ZRS") [97]. Initially, FMIRO were ascribed to multiphoton processes [95, 99]. This expanation, however, failed to reproduce the observations [98], where the FMIRO only occured at ω below a certain threshold value. It was shown that the threshold can be explained in the framework of the single-photon inelastic mechanism [98, 100]. Here, the FMIRO near combined resonances $n\omega = m\omega_c$ occured due to a resonant series of n single-photon transitions with *real* absorption (emission) of the microwave quanta [100], in distinction to the virtual multiphoton processes. A systematic theory of the FMIRO [101] has shown that the existing theories [99, 100] miss several important contributions. In particular, in the limit of well separated LLs the FMIRO are dominated by multiphoton inelastic mechanism. Provided $\tau_{\rm in}/\tau_{\rm q} \gg 1$, the multiphoton displacement mechanism [99] yields a parametrically smaller contribution and can be neglected. At weaker magnetic field the effects related to microwave-induced sidebands in the DOS become important. Close to the magnetic field at which the LLs start to overlap, the FMIRO are dominated by the single-photon inelastic mechanism [100]. Finally, in the regime of strongly overlapping LLs the FMIRO get exponentially suppressed.

A unified picture of the photoresponce in the limit of overlapping LLs was recently developed in [102]. On top of nonlinear interplay between the inelastic and displacement mechanisms at elevated microwave power, two novel mechanisms leading to the MIRO, "quadrupole" and "photovoltaic", were identified. In the quadrupole mechanism, the microwave radiation leads to excitation of the second angular harmonic of the distribution function. The dc response in the resulting nonequilibrium state yields an oscillatory contribution to the Hall part of the photoconductivity tensor which violates Onsager symmetry. In the photovoltaic mechanism, a combined action of the microwave and dc fields produces non-zero temporal harmonics of the stationary distribution function. The ac response in this state contributes to both the longitudinal and Hall MIRO. Provided $\tau_{\rm in}/\tau_{\rm q} \gg 1$, the inelastic mechanism still gives the dominant contribution to the diagonal part of the photoconductivity tensor. However, the quadrupole and photovoltaic mechanisms are the only ones yielding oscillatory corrections to the Hall part. Further, it was shown that a competition between various nonlinear effects (the feedback effects, the excitation of high angular and temporal harmonics of the distribution function, and the multiphoton effects) drives the system through four different nonlinear regimes with increasing microwave power. Most dramatic changes in the photoresponse are due to the feedback effects. At $\mathcal{P}_\omega \gg 1$, the feedback from the microwave–induced oscillations of the isotropic part of the distribution $f(\varepsilon)$ leads to the saturation of the inelastic contribution, and to the strong interplay of the inelastic effect and all other contributions to the MIRO. In particular, the strong oscillations of $f(\varepsilon)$ change sign of the most relevant parts of the displacement and photovoltaic contributions. At higher power, $\mathcal{P}_\omega \gg \omega_c\tau_{\rm in}$, the feedback suppresses the effects on higher temporal and angular harmonics of the distribution function. At still higher power, $\mathcal{P}_\omega \gg \tau_{\rm in}/\tau_{\rm q}$, the multiphoton excitation becomes pronounced and starts to compete with the feedback effects. Finally, at $\mathcal{P}_\omega \gg \tau_{\rm in}/\omega_c^2\tau_{\rm q}^3$, the feedback and multiphoton effects destroy all quantum contributions, restoring the classical Drude conductivity.

7.5 New developments and open questions

In spite of the essential advances in the understanding of nonequilibrium magnetotransport phenomena in a 2DEG, a number of questions remain open. A puzzling insensitivity of the MIRO to the direction of circular polarization of the microwave field was reported in [103]. The strong interplay [104] between the dc– [105, 106] and microwave–induced oscillations deserves theoretical study. A further challenging direction of future experimental and theoretical research is the transition to the ZRS, the domain structure, electron transport and noise in the ZRS; first steps in this direction have been made in [107, 108]. In particular, the theory has not explained the seemingly activated temperature dependence of the residual resistance in the ZRS. Recently discovered B-periodic magnetooscillations [109] which were ascribed to the microwave excitation of 2D edge magnetoplasmons warrant further investigation; in particular, their microscopic mechanism is still unclear.

Acknowledgements Most of the work reported in this review has been done in the framework of the Schwerpunktprogramm “Quanten-Hall-Systeme” of the Deutsche Forschungsgemeinschaft. We acknowledge collaboration with Y. Adamov, I.L. Aleiner, S.I. Dorozhkin, O. Entin-Wohlman, Y. Levinson, I.V. Pechenezhskii, E. Tsitsishvili, M.G. Vavilov, F. von Oppen, and J. Wilke on topics reviewed in this article. We are grateful to P.T. Coleridge, W. Dietsche, S.I. Dorozhkin, R.R. Du, A.V. Germanenko, M.E. Gershenson, R. Haug, I.V. Kukushkin, Z.D. Kvon, J.G.S. Lok, R.G. Mani, G.M. Minkov, C. Mitzkus, E.B. Olshanetsky, V.M. Pudalov, V. Renard, A.K. Savchenko, J.H. Smet, K. von Klitzing, D. Weiss, and M.A. Zudov for informing us on the experimental results and for stimulating discussions. We also acknowledge support by the DFG Center for Functional Nanostructures, by EUROHORCS/ESF (I.V.G.), as well as by the INTAS Project 05-1000008-8044.

References

[1] C.W.J. Beenakker and H. van Houten, Solid State Phys. **44**, 1 (1991).
[2] D.K. Ferry and S.M. Goodnick, *Transport in Nanostructures* (Cambridge University Press, 1997).
[3] D.V. Khveshchenko, Phys. Rev. Lett. **77**, 1817 (1996).
[4] A.D. Mirlin, D.G. Polyakov, and P. Wölfle, Phys. Rev. Lett. **80**, 2429 (1998).
[5] A.D. Mirlin, J. Wilke, F. Evers, D.G. Polyakov, and P. Wölfle, Phys. Rev. Lett. **83**, 2801 (1999).
[6] M.M. Fogler, A.Yu. Dobin, V.I. Perel, and B.I. Shklovskii, Phys. Rev. B **56**, 6823 (1997).
[7] B.I. Halperin, P.A. Lee, and N. Read, Phys. Rev. B **47**, 7312 (1993).
[8] F. Evers, A.D. Mirlin, D.G. Polyakov, and P. Wölfle, Phys. Rev. B **60**, 8951 (1999).
[9] See, e.g., J.H. Smet, in *Composite Fermions*, edited by O. Heinonen (Singapore, World Scientific, 1998).
[10] M. Dyakonov and R. Jullien, private communication.
[11] G.M. Gusev, P. Basmaji, Z.D. Kvon, L.V. Litvin, Yu.V. Nastaushev, and A.I. Toropov, J. Phys.: Condens. Matter **6**, 73 (1994).
[12] K. Tsukagoshi, S. Wakayama, K. Oto, S. Takaoka, K. Murase, and K. Gamo, Phys. Rev. B **52**, 8344 (1995).
[13] G. Lütjering, Ph.D. Thesis (Stuttgart University, 1996).
[14] G. Nachtwei, Z.H. Liu, G. Lütjering, R.R. Gerhardts, D. Weiss, K. von Klitzing, and K. Eberl, Phys. Rev. B **57**, 9937 (1998).
[15] S. Cinà, D.D. Arnone, H.P. Hughes, C.L. Foden, D.M. Whittaker, M. Pepper, and D.A. Ritchie, Phys. Rev. B **60**, 7780 (1999).
[16] O. Yevtushenko, G. Lütjering, D. Weiss, and K. Richter, Phys. Rev. Lett. **84**, 542 (2000).
[17] P.T. Coleridge, Phys. Rev. B **44**, 3793 (1991).
[18] T. Saku, Y. Horikoshi, and Y. Tokura, Jpn. J. Appl. Phys. **35**, 34 (1996).
[19] V. Umansky, R. de Picciotto, and M. Heiblum, Appl. Phys. Lett. **71**, 683 (1997).
[20] D.G. Polyakov, F. Evers, A.D. Mirlin, and P. Wölfle, Phys. Rev. B **64**, 205306 (2001).
[21] A.D. Mirlin, D.G. Polyakov, F. Evers, and P. Wölfle, Phys. Rev. Lett. **87**, 126805 (2001).
[22] E.M. Baskin, L.N. Magarill, and M.V. Entin, Sov. Phys. JETP **48**, 365 (1978); E.M. Baskin and M.V. Entin, Physica B **249**, 805 (1998).

[23] A.V. Bobylev, F.A. Maaø, A. Hansen, and E. H. Hauge, Phys. Rev. Lett. **75**, 197 (1995); A.V. Bobylev, F.A. Maaø, A. Hansen, and E. H. Hauge, J. Stat. Phys. **87**, 1205 (1997).
[24] A. Kuzmany and H. Spohn, Phys. Rev. E **57**, 5544 (1998).
[25] A. Dmitriev, M. Dyakonov, and R. Jullien, Phys. Rev. B **64**, 233321 (2001).
[26] A. Dmitriev, M. Dyakonov, and R. Jullien, Phys. Rev. Lett. **89**, 266804 (2002); V.V. Cheianov, A.P. Dmitriev, V.Yu. Kachorovskii, Phys. Rev. B **68**, 2013 04 (2003); *ibid* **70** 245307 (2004).
[27] M.H. Ernst and A. Weyland, Phys. Lett. A **34**, 39 (1971).
[28] M.B. Isichenko, Rev. Mod. Phys. **64**, 961 (1992).
[29] J. Smet, private communication; M. Heiblum and V. Umansky, private communication.
[30] J. Wilke, A.D. Mirlin, D.G. Polyakov, F. Evers, and P. Wölfle, Phys. Rev. B **61**, 13774 (2000).
[31] F. Evers, A.D. Mirlin, D.G. Polyakov, and P. Wölfle, Sov. Phys. Uspekhi (Suppl.) **171**, 27 (2001).
[32] D.G. Polyakov, F. Evers, and I.V. Gornyi, Phys. Rev. B **65**, 125326 (2002).
[33] I.A. Dmitriev, A.D. Mirlin, and D.G. Polyakov, Phys. Rev. B **70**, 165305 (2004).
[34] D. Weiss, K. v. Klitzing, K. Ploog, and G. Weimann, Europhys. Lett. **8**, 179 (1989).
[35] C. W. J. Beenakker, Phys. Rev. Lett. **62**, 2020 (1989).
[36] R.R. Gerhardts, D. Weiss, and K. von Klitzing, Phys. Rev. Lett. **62**, 1173 (1989); R. W. Winkler, J. P. Kotthaus, and K. Ploog, *ibid*. **62**, 1177 (1989); P. Vasilopoulos and F.M. Peeters, *ibid*. **63**, 2120 (1989).
[37] A.D. Mirlin and P. Wölfle, Phys. Rev. B **58**, 12986 (1998).
[38] Y. Levinson, O. Entin-Wohlman, A. D. Mirlin, and P. Wölfle, Phys. Rev. B **58**, 7113 (1998).
[39] A. D. Mirlin, P. Wölfle, Y. Levinson, and O. Entin-Wohlman, Phys. Rev. Lett. **81**, 1070 (1998).
[40] F. von Oppen, A. Stern, and B. I. Halperin, Phys. Rev. Lett. **80**, 4494 (1998).
[41] S. D. M. Zwerschke and R. R. Gerhardts, Phys. Rev. Lett. **83**, 2616 (1999).
[42] J. H. Smet, K. von Klitzing, D. Weiss, W. Wegscheider, Phys. Rev. Lett. **80**, 4538 (1998).
[43] J. H. Smet, S. Jobst, K. von Klitzing, D. Weiss, W. Wegscheider, and V. Umansky, Phys. Rev. Lett. **83**, 2620 (1999).
[44] A.D. Mirlin, E. Tsitsishvili, and P. Wölfle, Phys. Rev. B **63**, 245310 (2001).
[45] A.D. Mirlin, E. Tsitsishvili, and P. Wölfle, Phys. Rev. B **64**, 125319 (2001).
[46] R. Menne and R. R. Gerhardts, Phys. Rev. B **57**, 1707 (1998).
[47] P. H. Beton, E. S. Alves, P. C. Main, L. Eaves, M. W. Dellow, M. Henini, O. H. Hughes, S. P. Beaumont, and C. D. W. Wilkinson, Phys. Rev. B **42**, 9229 (1990).
[48] V.D. Fil', V.I. Denisenko, and P.A. Bezuglyi, Fiz. Nizk. Temp. **1**, 1217 (1975) [Sov. J. Low Temp. Phys. **1**, 584 (1975)].
[49] Yu.M. Galperin, V.L. Gurevich, and V.I. Kozub, Usp. Fiz. Nauk **128**, 107 (1979) [Sov. Phys. Usp. **22**, 352 (1979)] and references therein.
[50] C. Albrecht, J.H. Smet, D. Weiss, K. von Klitzing, R. Hennig, M. Langenbuch, M. Suhrke, U. Rössler, V. Umansky, and H. Schweizer, Phys. Rev. Lett. **83**, 2234 (1999).
[51] B.L. Altshuler and A.G. Aronov, *Electron-electron interactions in disordered conductors*, edited by A.L. Efros and M. Pollak (Elsevier, 1985)
[52] A. Houghton, J.R. Senna, and S.C. Ying, Phys. Rev. B **25**, 2196 (1982).
[53] E. Abrahams, S.V. Kravchenko, and M.P. Sarachik, Rev. Mod. Phys. **73**, 251 (2001).
[54] B.L. Altshuler, D.L. Maslov, and V.M. Pudalov, Physica E **9** (2), 209 (2001).
[55] G.Zala, B.N.Narozhny, and I.L.Aleiner, Phys. Rev. B **64**, 214204 (2001); *ibid*, **65**, 201201 (2001); *ibid*, **65**, 020201 (2002).
[56] I.V. Gornyi and A.D. Mirlin, Phys. Rev. Lett. **90**, 076801 (2003); Phys. Rev. B **69**, 045313 (2004).
[57] L. Li, Y.Y. Proskuryakov, A.K. Savchenko, E.H. Linfield, and D.A. Ritchie, Phys. Rev. Lett. **90**, 076802 (2003).
[58] E.B. Olshanetsky, V. Renard, Z.D. Kvon, J.C. Portal, N.J. Woods, J. Zhang, and J.J Harris, Phys. Rev. B **68**, 085304 (2003).
[59] T. Ando, J. Phys. Soc. Japan **38**, 989 (1975); T. Ando, A.B. Fowler, and F. Stern, Rev. Mod. Phys. **54**, 437 (1982).
[60] The consideration of ultra-long-range disorder with $d \gg l_B$ in [59] is not justified since this condition violates the applicability of SCBA.
[61] I.A. Dmitriev, A.D. Mirlin, and D.G. Polyakov, Phys. Rev. Lett. **91**, 226802 (2003).
[62] M.E. Raikh and T.V. Shahbazyan, Phys. Rev. B **47**, 1522 (1993); B. Laikhtman and E.L. Altshuler, Ann. Phys. **232**, 332 (1994).
[63] P.T. Coleridge, R. Stoner, and R. Fletcher, Phys. Rev. B **39**, 1120 (1989).
[64] Y. Adamov, I.V. Gornyi, and A.D. Mirlin, Phys. Rev. B **73**, 045426 (2006).
[65] J. M. Luttinger and J. C. Ward, Phys. Rev. **118**, 1417 (1960).

[66] A.A. Abrikosov, L.P. Gorkov, and I.E. Dzyaloshinski, *Methods of quantum field theory in statistical physics*, (Dover Publications, New York,1963).
[67] J.M. Luttinger, Phys. Rev. **121**, 1251 (1961).
[68] G.M. Martin, D.L. Maslov, and M.Yu. Reizer, Phys. Rev. B **68**, 241309(R) (2003).
[69] M. Fowler and R. E. Prange, Physics **1**, 315 (1965); S. Engelsberg and G. Simpson, Phys. Rev. B **2**, 1657 (1970).
[70] T.J. Gramila, J.P. Eisenstein, A.H. MacDonald, L.N. Pfeiffer, and K.W. West, Phys. Rev. Lett. **66**, 1216 (1991); Phys. Rev. B **47**, 12957 (1993).
[71] U. Sivan, P.M. Solomon, and H. Shtrikman, Phys. Rev. Lett. **68**, 1196 (1992).
[72] N.P.R. Hill, J.T. Nicholls, E.H. Linfield, M. Pepper, D.A. Ritchie, A.R. Hamilton, and G.A.C. Jones, J. Phys.: Condens. Matter **8**, L557 (1996).
[73] H. Rubel, A. Fisher, W. Dietsche, K. von Klitzing, and K. Eberl, Phys. Rev. Lett. **78**, 1763 (1997).
[74] X.G. Feng, S. Zelakiewicz, H. Noh, T.J. Ragucci, and T.J. Gramila, Phys. Rev. Lett. **81**, 3219 (1998).
[75] M.P. Lilly, J.P. Eisenstein, L.N. Pfeiffer, and K.W. West, Phys. Rev. Lett. **80**, 1714 (1998).
[76] M. Kellogg, I.B. Spielman, J.P. Eisenstein, L.N. Pfeiffer, and K.W. West, Phys. Rev. Lett. **88**, 126804 (2002).
[77] M. Kellogg, J.P. Eisenstein, L.N. Pfeiffer, and K.W. West, Phys. Rev. Lett. **90**, 246801 (2003).
[78] J.G.S. Lok, S. Kraus, M. Pohlt, W. Dietsche, K. von Klitzing, W. Wegscheider, and M. Bichler, Phys. Rev. B **63**, 041305 (2001).
[79] K. Muraki, J.G.S. Lok, S. Kraus, W. Dietsche, K. von Klitzing, D. Schuh, M. Bichler, and W. Wegscheider, Phys. Rev. Lett. **92**, 246801 (2004).
[80] L.Zheng, and A.H. MacDonald, Phys. Rev. B **48**, 8203 (1993).
[81] F. von Oppen, S.H. Simon, and A. Stern, Phys. Rev. Lett. **87**, 106803 (2001).
[82] I.V. Gornyi, A.D. Mirlin, and F. von Oppen, Phys. Rev. B **70**, 245302 (2004).
[83] M.A. Zudov, R.R. Du, J.A. Simmons, and J.R. Reno, Phys. Rev. B **64**, 201311(R) (2001).
[84] R.G. Mani, J.H. Smet, K. von Klitzing, V. Narayanamurti, W.B. Johnson, and V. Umansky, Nature **420**, 646 (2002).
[85] M.A. Zudov, R.R. Du, L.N. Pfeiffer, and K.W. West, Phys. Rev. Lett. **90**, 046807 (2003).
[86] A.C. Durst, S. Sachdev, N. Read, and S.M. Girvin, Phys. Rev. Lett. **91**, 086803 (2003).
[87] V.I. Ryzhii, Sov. Phys. Solid State **11**, 2078 (1970); V.I. Ryzhii, R.A. Suris, and B.S. Shchamkhalova, Sov. Phys. Semicond. **20**, 1299 (1986).
[88] M.G. Vavilov and I.L. Aleiner, Phys. Rev. B 69, 035303 (2004).
[89] A.V. Andreev, I.L. Aleiner, and A.J. Millis, Phys. Rev. Lett. **91**, 056803 (2003).
[90] I.A. Dmitriev, M.G. Vavilov, I.L. Aleiner, A.D. Mirlin, and D.G. Polyakov, Physica E 25, 205 (2004).
[91] I.A. Dmitriev, M.G. Vavilov, I.L. Aleiner, A.D. Mirlin, and D.G. Polyakov, Phys. Rev. B 71, 115316 (2005).
[92] S.I. Dorozhkin, JETP Lett. **77**, 577 (2003).
[93] R.L. Willett, L.N. Pfeiffer, and K.W. West, Phys. Rev. Lett. **93**, 026804 (2004).
[94] M.G. Vavilov, I.A. Dmitriev, I.L. Aleiner, A.D. Mirlin, and D.G. Polyakov, Phys. Rev. B **70**, 161306(R) (2004).
[95] M.A. Zudov, Phys. Rev. B **69**, 041304(R) (2004).
[96] S.I. Dorozhkin, J.H. Smet, V. Umansky, and K. von Klitzing, Phys. Rev. B **71**, 201306(R) (2005).
[97] M.A. Zudov, R.R. Du, L.N. Pfeiffer, and K.W. West, Phys. Rev. B **73**, 041303(R) (2006).
[98] S.I. Dorozhkin, J.H. Smet, K. von Klitzing, L.N. Pfeiffer, and K.W. West, cond-mat/0608633.
[99] X.L. Lei and S.Y. Liu, Appl. Phys. Lett. **88**, 212109 (2006).
[100] I.V. Pechenezhskii, S.I. Dorozhkin, and I.A. Dmitriev, JETP Lett. **85**, 86 (2007).
[101] I.A. Dmitriev, A.D. Mirlin, and D.G. Polyakov, Phys. Rev. Lett. **99**, 206805 (2007).
[102] I.A. Dmitriev, A.D. Mirlin, and D.G. Polyakov, Phys. Rev. B. **75**, 245320 (2007).
[103] J.H. Smet, B. Gorshunov, C. Jiang, L. Pfeiffer, K. West, V. Umansky, M. Dressel, R. Meisels, F. Kuchar, and K. von Klitzing, Phys. Rev. Lett. **95**, 116804 (2005).
[104] W. Zhang, M.A. Zudov, L.N. Pfeiffer, and K.W. West, Phys. Rev. Lett. **98**, 106804 (2007).
[105] C.L. Yang, J. Zhang, R.R. Du, J.A. Simmons, and J.L. Reno, Phys. Rev. Lett. **89**, 076801 (2002).
[106] M.G. Vavilov, I.L. Aleiner, and L.I. Glazman, Phys. Rev. B **76**, 115331 (2007).
[107] A. Auerbach, I. Finkler, B.I. Halperin, and A. Yacoby, Phys. Rev. Lett. **94**, 196801 (2005).
[108] J. Alicea, L. Balents, M.P.A. Fisher, A. Paramekanti, and L. Radzihovsky, Phys. Rev. B **71**, 235322 (2005).
[109] I.V. Kukushkin, M.Yu. Akimov, J.H. Smet, S.A. Mikhailov, K. von Klitzing, I.L. Aleiner, V.I. Falko, Phys. Rev. Lett. **92**, 236803 (2004).